Kinetochore Function and Chromosome Segregation Rely on Critical Residues in Histones H3 and H4 in Budding Yeast

Tessie M. Ng,*,† Tineke L. Lenstra,‡ Nicole Duggan,* Shuangying Jiang,§ Steven Ceto,* Frank C. P. Holstege,‡ Junbiao Dai,§ Jef D. Boeke, and Sue Biggins*,[1]**

*Division of Basic Sciences, Fred Hutchinson Cancer Research Center, Seattle, Washington 98109, †Molecular and Cellular Biology Program, University of Washington, Seattle, Washington 98195, ‡Molecular Cancer Research, University Medical Centre Utrecht, CG Utrecht 3584, The Netherlands, §School of Life Sciences, Tsinghua University, Beijing 100084, China, and **High Throughput Biology Center, Johns Hopkins University School of Medicine, Baltimore, Maryland 21205

ABSTRACT Accurate chromosome segregation requires that sister kinetochores biorient and attach to microtubules from opposite poles. Kinetochore biorientation relies on the underlying centromeric chromatin, which provides a platform to assemble the kinetochore and to recruit the regulatory factors that ensure the high fidelity of this process. To identify the centromeric chromatin determinants that contribute to chromosome segregation, we performed two complementary unbiased genetic screens using a library of budding yeast mutants in every residue of histone H3 and H4. In one screen, we identified mutants that lead to increased loss of a nonessential chromosome. In the second screen, we isolated mutants whose viability depends on a key regulator of biorientation, the Aurora B protein kinase. Nine mutants were common to both screens and exhibited kinetochore biorientation defects. Four of the mutants map near the unstructured nucleosome entry site, and their genetic interaction with reduced *IPL1* can be suppressed by increasing the dosage of *SGO1*, a key regulator of biorientation. In addition, the composition of purified kinetochores was altered in six of the mutants. Together, this work identifies previously unknown histone residues involved in chromosome segregation and lays the foundation for future studies on the role of the underlying chromatin structure in chromosome segregation.

IT is critical to understand the mechanisms that ensure accurate chromosome segregation because errors are associated with diseases such as cancer and can lead to cell death (Williams and Amon 2009; Compton 2011). Proper chromosome segregation is a highly regulated process that requires the coordination of a number of events. After DNA replication, sister chromatids are physically linked by cohesion (Oliveira and Nasmyth 2010; Nasmyth 2011). Kinetochores, the macromolecular complexes that assemble on centromeric DNA, must biorient and attach to microtubules from opposite poles. Once bioriented attachments are made, sister kinetochores come under tension due to microtubule-pulling forces on linked sister chromatids. Kinetochores lacking tension trigger the spindle checkpoint until proper attachments are made (Nezi and Musacchio 2009). Once every pair of sister chromatids has made bioriented attachments at metaphase, cohesion is dissolved, allowing sister chromatids to segregate to opposite poles at anaphase.

A key regulator of biorientation is the conserved chromosomal passenger complex (CPC), an essential protein kinase complex that detects and corrects microtubule–kinetochore attachments that are not under tension (Lampson and Cheeseman 2011). Phosphorylation of kinetochore substrates by the CPC protein kinase Aurora B destabilizes such aberrant attachments, giving the cell another opportunity to make proper, bioriented attachments (Liu and Lampson 2009). The CPC localizes to the inner centromere (Cooke *et al.* 1987), consistent with the model that tension between sister kinetochores stabilizes bioriented attachments by moving key substrates at the outer kinetochore away from the CPC (Tanaka *et al.* 2002; Fuller *et al.* 2008; Liu *et al.* 2009). However, the precise mechanism by which the CPC acts on attachments not under tension is still unclear

doi: 10.1534/genetics.113.152082
Manuscript received April 8, 2013; accepted for publication September 5, 2013
Supporting information is available online at http://www.genetics.org/lookup/suppl/doi:10.1534/genetics.113.152082/-/DC1.
[1]Corresponding author: Fred Hutchinson Cancer Research Center, 1100 Fairview Ave. N, A2-168, P. O. Box 19024, Seattle, WA 98109. E-mail: sbiggins@fhcrc.org

(Maresca and Salmon 2010). The Aurora B kinase is also required for the spindle checkpoint when kinetochores lack tension (Biggins and Murray 2001), although it is controversial whether this function is due to its role in destabilizing kinetochore–microtubule attachments (Musacchio 2011).

Another conserved protein implicated in biorientation and the tension checkpoint is shugoshin. Although the shugoshin family is well known for its meiotic role in protecting centromeric cohesion (Watanabe 2005; Gutierrez-Caballero *et al.* 2012), some family members also facilitate kinetochore biorientation and the checkpoint response to the lack of tension during mitosis (Indjeian *et al.* 2005; Vaur *et al.* 2005; Indjeian and Murray 2007; Kiburz *et al.* 2008). A conserved requirement for shugoshin localization to centromeres and pericentromeres is the phosphorylation of H2A S121 by the Bub1 protein kinase (Kawashima *et al.* 2010). In budding yeast, shugoshin (Sgo1) recruitment to nucleosomes also requires residue G44 in H3, which resides near H2A S121 in the nucleosome structure (Luger *et al.* 1997; Luo *et al.* 2010). In many organisms, there is an interdependence between shugoshin and Aurora B localization and activity (Dai *et al.* 2006; Resnick *et al.* 2006; Kawashima *et al.* 2007, 2010; Vanoosthuyse *et al.* 2007; Kelly *et al.* 2010; Wang *et al.* 2010; Yamagishi *et al.* 2010; Storchova *et al.* 2011), consistent with their close association with chromatin.

The underlying foundation of kinetochores is a specialized chromatin structure that creates the epigenetic mark for kinetochores and contributes to their assembly and function. While the bulk of the genome contains nucleosomes with ~147 bp of DNA wrapped around two copies each of histone H2A, H2B, H3, and H4, the centromere contains a specialized histone H3 variant called Cenp-A (Maddox *et al.* 2012). In most organisms, Cenp-A nucleosomes are interspersed with H3 nucleosomes in the core centromere and flanked by H3 nucleosomes in heterochromatin (Blower *et al.* 2002; Cam *et al.* 2005). In budding yeast, there is a single Cenp-A nucleosome positioned at the centromere (Meluh *et al.* 1998; Furuyama and Biggins 2007; Krassovsky *et al.* 2012), as well as additional Cenp-A in the flanking pericentromeric chromatin (Lawrimore *et al.* 2011; Henikoff and Henikoff 2012). While budding yeast pericentromeres lack heterochromatin, a conserved feature is the enrichment of cohesin and Sgo1 to promote kinetochore biorientation (Blat and Kleckner 1999; Tanaka *et al.* 1999; Kiburz *et al.* 2005, 2008; Eckert *et al.* 2007). In addition, evidence suggests that the pericentromeric chromatin adopts a specialized intramolecular structure that is organized by Sgo1 and facilitates biorientation in budding yeast (Yeh *et al.* 2008; Haase *et al.* 2012). Consistent with this, changes in pericentromeric chromatin composition lead to defects in the organization of inner kinetochore proteins and chromosome segregation (Chambers *et al.* 2012; Verdaasdonk *et al.* 2012).

While it is clear that a specialized chromatin structure facilitates the assembly and function of >38 core kinetochore proteins and additional regulatory proteins (Stellfox *et al.* 2012; Valente *et al.* 2012), the key determinants of this chromatin structure have still not been fully elucidated. We therefore set out to identify histone H3 and H4 residues that contribute to chromosome segregation and kinetochore biorientation by performing two systematic genetic screens in budding yeast. Our work identifies key residues in both histones that were previously not known to regulate segregation, some of which contribute to Sgo1 function. This work lays the foundation for future studies aimed at understanding the roles of centromeric and pericentromeric chromatin in chromosome segregation and genomic stability.

Materials and Methods

Screen to identify mutants sensitive to decreased IPL1 function

Individual mutations were integrated at the endogenous *HHT2-HHF2* locus as described previously (Dai *et al.* 2008). H3 mutations were integrated into SBY9120 and H4 mutations into SBY9119. Correct integration was verified by PCR using the primers SB2409 and SB2410 for H3 mutants, and SB2409 and SB2411 for H4 mutants. Integrations were attempted at least three times before a given mutant was not pursued (Supporting Information, Table S1). The absence of the endogenous wild-type (WT) locus was also confirmed using the primers SB2409 and SB2412. Fivefold serial dilutions of asynchronously growing cells were grown for 2–3 days on YPD plates in the presence and absence of 25 μg/ml doxycycline or 15 μg/ml benomyl. Primer sequences are available upon request.

Chromosome loss assays

The yeast strain (JDY176) used for testing chromosome loss was derived from SBY8053, which contains an artificial chromosome III fragment with *SUP11* and *HIS3* markers (Hieter *et al.* 1985). The *HHT1-HHF1*-coding fragment, including the promoter, was knocked out to generate JDY168. The *ura3-1* mutation was corrected to obtain *URA3* strains followed by deletion of the ORF to generate an *ura3Δ0* strain as described (Brachmann *et al.* 1998). The resultant strain, JDY176, was used in subsequent studies.

Individual histone mutations were integrated at the endogenous *HHT2-HHF2* locus as described previously (Dai *et al.* 2008). Correct integration was confirmed by PCR, and at least two independent isolates were obtained for each mutant (primers SB2409, SB2410, SB2411, SB2412). Each mutant was streaked onto synthetic complete agar plates containing 48 μM adenine and grown at 30° for 4 days. The plates were stored at 4° for 3 days before evaluating the percentage of colonies with red sectors. For quantification of chromosome loss, the yeast strains were grown in liquid medium overnight. The cell density in the culture was measured and ~200 cells were plated onto synthetic complete agar plates containing 48 μM adenine. The number of colonies containing at least half red sectors was quantified and divided by the total number of colonies to

calculate the percentage of chromosome loss in the first generation.

Microbial techniques and plasmid construction

Media and microbial techniques were as described (Sherman *et al.* 1974; Rose *et al.* 1990). All experiments were performed at 23° unless otherwise noted. In all synchronous cell-cycle experiments reported, 1 or 10 μg/ml α-factor (custom synthesized by United Biochemical Research, Inc., Seattle) was used to arrest *bar1-1* and *BAR1* cells in G1, respectively. Doxycycline (Sigma-Aldrich, St. Louis) was used at 25 μg/ml. Yeast strains are listed in Table S3. High-copy *SGO1* (pSB1780) or control [pRS425, (Sikorski and Hieter 1989)] plasmids were introduced into the histone mutant strains by transformation.

To generate a high-copy *SGO1* plasmid with the *LEU2* marker (pSB1780), the *URA3* 2-μm plasmid pMK573 (Luo *et al.* 2010) was digested with *Hpa*I and *Aat*II to remove *URA3*. The *LEU2* gene was isolated from YEplac181 (Gietz and Sugino 1988) by digestion with the same restriction enzymes and ligated to the digested plasmid pMK573 to create pSB1780.

Flow cytometry

For the *orc2-1* experiment, WT and *orc2-1* strains were shifted to 37° for 3 hr. For the histone mutant strains, cells were grown at room temperature. After harvesting cells, they were fixed with 70% ethanol at room temperature. Fixed cells were then incubated in 0.2 mg/ml RNase A (Sigma-Aldrich) in 50 mM Tris–HCl, pH 8.0, for 4 hr at 37° and 2 mg/ml Proteinase K (Roche, Indianapolis) in 50 mM Tris, pH 7.5, for 1 hr at 50°. Cells were then incubated with 5 mM Sytox Green (Molecular Probes, Eugene, OR) in 50 mM Tris, pH 7.5. Data were collected and analyzed using Cell Quest software (BD Biosciences, San Jose, CA).

Microscopy, protein, and immunological techniques

Analysis of GFP-*Lac*I was performed as described (Biggins *et al.* 1999). For all microscopy experiments, >200 cells were scored. The Bernoulli distribution was used to assess statistical significance at 95% confidence. Anaphase was analyzed by staining cells with 4′,6-diamidino-2-phenylindole (Sigma-Aldrich) and identifying cells with two separated DNA masses. Protein extracts were made and immunoblotted as described (Minshull *et al.* 1996). Quantitative immunoblotting was performed with IRDye secondary antibodies from LI-COR at a 1:15,000 dilution. The immunoblots were imaged on a LI-COR imaging system, and the protein levels were quantified using the ImageJ program. The mean of three independent experiments is reported. Loading controls for all experiments were either anti-tubulin (Accurate Chemical and Scientific) used at 1:1000, or anti-PGK1 (Invitrogen) at a 1:10,000 dilution. Centromeric minichromosomes were purified and analyzed by immunoblotting as described previously (Akiyoshi *et al.* 2009). Anti-Spc105 polyclonal antibodies were used at a 1:1000 dilution (Akiyoshi *et al.* 2010), anti-FLAG monoclonal antibodies (Sigma-Aldrich) were used at 1:3000, and anti-Cse4 polyclonal antibodies at 1:500 (Pinsky *et al.* 2003). Anti-Ndc80 (OD4, 1:10,000), anti-Ndc10 (OD1, 1:5,000), anti-Mif2 (OD2, 1:6,000), and anti-Ctf19 (OD10, 1:15,000) polyclonal antibodies were a generous gift from Arshad Desai (Akiyoshi *et al.* 2009).

Chromatin immunoprecipitation assays and quantitative real-time PCR

Chromatin immunoprecipitation (ChIP) was performed using antibodies against Cse4 as described previously (Collins *et al.* 2005), and samples were quantified by quantitative real-time PCR (7900HT, ABI Prism). DNA samples were amplified using a SYBR PCR mix (Applied Biosystems) at 95° for 10 min, 40 cycles of 95° for 15 sec, and 55° for 1 min using CEN3 (SB1253 and SB1254) and *PHO5*-specific primers (SB3063 and SB3064). PCR amplification efficiency and linearity were determined using serial dilutions of samples. Standard curves were generated for every PCR reaction and used for quantification of bound DNA that was expressed as the percentage of input DNA. Sequences of PCR primers are available upon request.

Nucleosome structures

Nucleosome structures were prepared with PyMOL (http://www.pymol.org/).

Expression profiling

Each mutant strain [derivatives of JDY86 as previously described (Dai *et al.* 2008)] was profiled four times from two independently inoculated cultures and harvested in early mid-log phase in SC medium with 2% glucose. Sets of mutants were grown alongside corresponding H3 and H4 WT cultures (single-copy H3 or H4) and processed in parallel. Dual-channel 70-mer oligonucleotide arrays were employed with a common reference WT RNA. All steps after RNA isolation were automated using robotic liquid handlers. These procedures were first optimized for accuracy (correct fold-change) and precision (reproducible result), using spiked-in RNA for calibration (van de Peppel *et al.* 2003). After quality control, normalization, and dye-bias correction (Margaritis *et al.* 2009), statistical analysis for mid-log cultures was performed for each mutant *vs.* the WT cells grown alongside using Limma. The reported fold-change is an average of the replicate mutant profiles *vs.* the H3 or H4 WT. Microarray data have been deposited in ArrayExpress under accession no. E-MTAB-1242 and in the Gene Expression Omnibus database under accession no. GSE39903.

Results

Identification of H3 and H4 residues important for chromosome segregation

To identify histone residues involved in the regulation of chromosome segregation, we screened for budding yeast H3

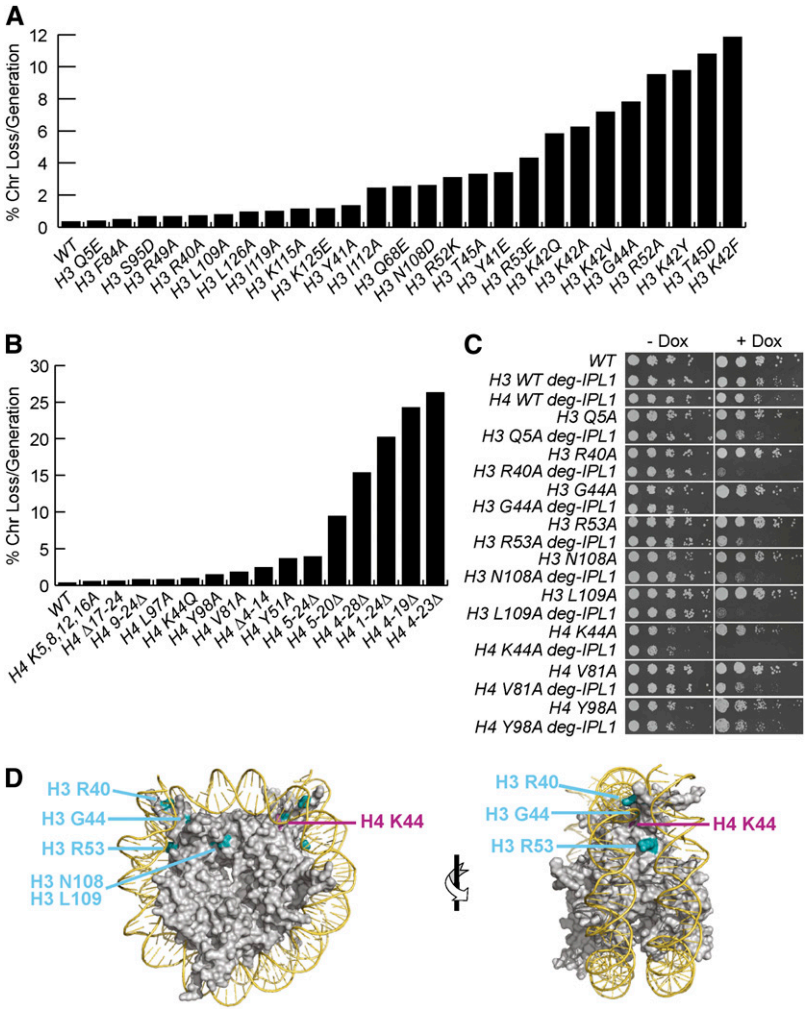

Figure 1 Identification of H3 and H4 mutants with chromosome segregation defects. (A and B) The frequency of chromosome loss for the indicated histone H3 (A) and H4 (B) mutants identified in the colony-sectoring assay is plotted [all strains are derived from JDY176 (Table S3)]. (C) Fivefold serial dilutions of strains containing the indicated histone mutant in the presence or absence of *deg-ipl1* (SBY719, SBY9837–SBY9847, SBY9880–SBY9888) were plated with (+) or without (−) doxycycline. Note that two different parent cassettes (WT H3 and H4) were used to generate mutants in the corresponding histone, and various pairs of images were cropped to assemble the figure. (D) The H3 (blue) and H4 residues (magenta) identified in both screens are highlighted on the nucleosome structure (Luger *et al.* 1997). The H3 Q5 residue in the unstructured tail and buried residues of H4 V81 and H4 Y98 are not shown. Front and side views are shown.

and H4 mutants that exhibit chromosome loss. We used a previously constructed library of mutants where every H3 and H4 amino acid was systematically changed to alanine and the modifiable residues were changed to both alanine and a charged residue (Dai *et al.* 2008). Deletions within the amino-terminal tails of each histone were also assayed. A cassette containing the mutants was introduced into the primary H3 and H4 locus, *HHT2-HHF2*, in a strain containing a deletion of the secondary H3 and H4 locus, *hht1-hhf1*Δ. The strain also contained an artificial chromosome fragment that allowed us to assay the frequency of chromosome loss using a colony color-sectoring assay (Hieter *et al.* 1985). Mutants that exhibited increased sectoring were quantified for the percentage of chromosome loss per generation. Together, 26 mutants in H3 and 15 mutants in H4 exhibited an increased frequency of chromosome loss compared to WT (Figure 1, A and B).

Histone mutations can cause pleiotropic effects, so we performed a second screen to identify the histone residues that might specifically contribute to kinetochore biorientation. We isolated mutants that require the full activity of the Ipl1/Aurora B protein kinase for viability. To do this, we used a previously characterized doxycycline-repressible degron allele, *deg-ipl1*, that targets the protein for degradation by the proteasome (Ng *et al.* 2009). Although *IPL1* is essential, doxycycline addition does not severely inhibit the growth of *deg-ipl1* cells (Figure 1C), indicating that these cells retain enough Ipl1 function to support viability. However, *deg-ipl1* is lethal when combined with other nonessential mutants such as the *mcm21* kinetochore mutant, indicating that it is a hypomorphic allele (Ng *et al.* 2009). We therefore introduced each alanine substitution mutation in H3 and H4 into a *deg-ipl1* strain containing a deletion of the secondary copy of H3 and H4, *hht1-hhf1*Δ. We note that 24 of the alanine mutants, including 6 of the residues identified in the chromosome loss screen (H3 Y41, H3 Q68, H3 L103, H3 I112, H3 I119, H4 L97), could not be generated in the *deg-ipl1* strain background, suggesting synthetic lethality, and could not be further pursued (Table S1). The remaining mutants were analyzed for growth in the presence and absence of doxycycline, and 29 mutants that exhibited some degree of sensitivity to down-regulation of *IPL1* compared to WT strains were identified (Table 1).

We focused on the mutants that were identified in both screens and are therefore most likely to be important for

Table 1 Summary of mutant phenotypes identified in the *deg-ipl1* and chromosome loss screens

Histone residue[a]	Location[b]	Chromosome loss[c]	Doxycycline sensitivity[d]	Increased temperature sensitivity[e]	Benomyl sensitivity[f]
H3 R2	T	—	±	+	R
H3 T3	T	—	±	−	+
H3 K4	T	—	+	+	R
H3 Q5	T	Q5E	+	−	+
H3 R26	T	—	±	±	+
H3 K36	T	—	±	−	+
H3 K37	T	—	±	ND	−
H3 R39	L	—	+	ND	R
H3 R40	L	R40A	+	+	+
H3 Y41	L	Y41A/E	NA	NA	NA
H3 K42	L	K42A/F/Q/V/Y	−	NA	−
H3 G44	L	G44A	++	ND	+++
H3 T45	L	T45A/D	+	ND	+++
H3 V46	L	—	+	+	±
H3 R49	L	R49A	−	NA	++
H3 R52	D	R52K/A	−	NA	++
H3 R53	D	R53E	±	+	±
H3 Q55	B	—	+	ND	+
H3 K56	L	—	+	ND	−
H3 T58	D	—	−	NA	+
H3 Q68	D	Q68E	NA	NA	NA
H3 E73	D	—	±	ND	++
H3 K79	D	—	−	NA	+
H3 L82	D	—	±	ND	±
H3 F84	L	F84A	−	NA	+++
H3 G90	D	—	−	−	++
H3 S95	B	S95D	−	−	−
H3 V101	B	—	±	ND	−
H3 L103	B	—	NA	NA	NA
H3 N108	B	N108D	+	+	−
H3 L109	B	L109A	++	+	+
H3 I112	D	I112A	NA	NA	NA
H3 K115	L	K115A	±	−	−
H3 I119	B	I119A	NA	NA	NA
H3 I124	B	—	+	ND	−
H3 K125	D	K125E	−	NA	−
H3 L126	D	L126A	−	NA	−
H3 L130	B	—	+	ND	++
H4 K20	D	—	−	NA	−
H4 I34	B	—	−	NA	−
H4 K44	L	K44Q	++	−	++
H4 Y51	D	Y51A	−	NA	−
H4 F61	D	—	++	ND	+++
H4 V81	B	V81A	++	+	+
H4 D85	B	—	+	ND	+
H4 L90	B	—	+	ND	+
H4 L97	B	L97A	NA	NA	NA
H4 Y98	B	Y98A	++	ND	++
H4 G99	B	—	−	NA	++
H4 Δ1-24	T	+	ND	ND	ND
H4 Δ4-14	T	+	ND	ND	ND
H4 Δ4-19	T	+	ND	ND	ND
H4 Δ4-23	T	+	ND	ND	ND
H4 Δ4-28	T	+	ND	ND	ND
H4 Δ5-20	T	+	ND	ND	ND
H4 Δ5-24	T	+	ND	ND	ND
H4 Δ9-24	T	+	ND	ND	ND
H4 Δ17-24	T	+	ND	ND	ND

NA, not applicable because the histone mutant could not be generated in the *deg-ipl1* strain background. ND, not determined.

[a] All histone residues assayed were mutated to alanine. In some cases, additional mutants were also assayed as indicated in the chromosome loss column.

[b] Locations as defined in Dai *et al.* (2008): T, tail; L, lateral; B, buried; D, disk.

[c] The indicated histone mutant exhibited increased chromosome loss relative to WT.

[d] "+" indicates sensitivity; "−" indicates no sensitivity.

[e] Indicated mutants were crossed to *ipl1-321* and assayed for genetic interaction based on increase temperature sensitivity. "+" indicates sensitivity; "−" indicates no sensitivity.

[f] "+" indicates sensitivity; "−" indicates no sensitivity. "R" indicates resistance compared to WT.

chromosome segregation. The corresponding residues are H3 Q5, H3 R40, H3 G44, H3 T45, H3 R53, H3 N108, H3 L109, H3 K115, and H4 K44, H4 V81, and H4 Y98. However, the H3 K115A mutant cells grew extremely slowly (data not shown), and the H3 T45A mutant cells were previously reported to have replication defects (Baker *et al.* 2010), so we did not continue to analyze them. The remaining nine mutants were assayed for the severity of their growth defect with or without the *deg-ipl1* allele by plating serial dilutions in the absence and presence of doxycycline (Figure 1C). In the absence of *IPL1* downregulation, all of the mutants grew well except H4 K44A and H4 Y98A. In the presence of doxycycline, the *H3 R40A*, *H3 G44A*, *H3 R53A*, *H3 N108A*, *H3 L109A*, *H4 K44A*, and *H4 V81A* mutants exhibited a strong or complete loss of viability, whereas the *H3 Q5A* and *H4 Y98A* mutants showed a weak dependence on full *IPL1* function. All of the identified residues are conserved, and mapping them onto the nucleosome structure shows that H3 R40, H3 G44, H3 R53, and H4 K44 cluster near the nucleosome entry/exit site, whereas H3 N108, H3 L109, H4 V81, and H4 Y98 are buried residues (Figure 1D) (Luger *et al.* 1997).

Analysis of replication and segregation in the histone mutant strains

Because chromosome-loss phenotypes can be a result of either replication or segregation defects, we performed fluorescence-activated cell sorting (FACS) on the histone mutants to analyze replication. As a control, we analyzed the *orc2-1* temperature-sensitive mutant that is defective in replication and shows an accumulation of cells with DNA content between 1N and 2N (Figure 2A). The *deg-ipl1 hht1-hhf1*Δ strains containing WT or mutant H3 or H4 were grown in the absence of doxycycline and processed for FACS (Figure 2B). None of the mutants exhibited a strong delay in S-phase, although subtle replication defects may exist that cannot be detected due to the resolution of this assay.

We next directly assayed chromosome segregation in each mutant strain by analyzing a fluorescently marked chromosome (Straight *et al.* 1996). Asynchronous cultures of *deg-ipl1* strains containing GFP-marked *Chromosome IV (ChrIV)*, and the H3 and H4 mutations were grown in doxycycline to repress *IPL1* for 6 hr. Cells that had proceeded through anaphase (segregated DNA to opposite poles) were scored for segregation of *ChrIV* to a single pole (missegregation) or opposite poles (accurate segregation) (Figure 3A). The strongest segregation defects occurred in the H3 R40A, H3 G44A, H3 L109A, H4 K44A, and H4 V81A mutant strains, which all exhibited >15% missegregation of *ChrIV* within 6 hr of *IPL1* downregulation. The H3 R53A and H3 N108A mutant strains showed a >10% missegregation defect after 6 hr, whereas there were no significant segregation defects in the H3 Q5A or H4 Y98A strains. Strikingly, the levels of chromosome missegregation in each mutant strain parallel the growth defects when *IPL1* is downregulated (see Figure 1B), suggesting that the loss of viability is due to chromosome missegregation.

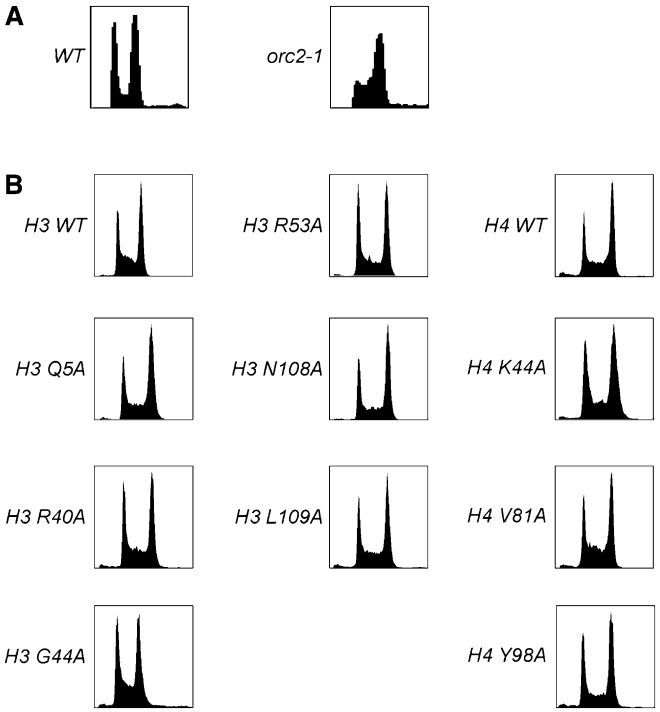

Figure 2 The histone mutants do not exhibit replication defects. (A) WT (SBY4) and *orc2-1* (SBY11682) strains were shifted to 37° and then subjected to FACS analysis. (B) FACS profiles of histone mutants that exhibit segregation defects. Asynchronous cultures of the indicated histone mutants (SBY9119, SBY9120, SBY9625, SBY9660, SBY9664, SBY9665, SBY9673, SBY9724, SBY9725, SBY9786, SBY9818, SBY9832) were processed for FACS analyses.

We next attempted to analyze segregation in a synchronous cycle by releasing cells from a G1 arrest into doxycyline. However, many of the histone mutants exhibited a transient delay in the onset of anaphase when released from G1 as indicated by the reduced percentage of cells with DNA masses at opposite poles relative to WT cells (data not shown). We reasoned that this delay could be due to spindle checkpoint activation, which would give sister chromatids additional time to biorient. We therefore examined *ChrIV* segregation in *deg-ipl1 mad3*Δ strains containing the histone mutations during a synchronous cell cycle. As expected, the absence of the spindle checkpoint reduced the delay in anaphase onset because >50% of the cells segregated their DNA to opposite poles within 80 min post-G1 release, similar to WT cells. *ChrIV* segregation was monitored at the time point (100 or 120 min after G1 release) when the highest percentage of cells had DNA masses at opposite poles (Figure 3B). Similar to our findings on asynchronous cells, there were significant segregation defects (>8%) in the H3 R40A, H3 N108A, H3 L109A, and the H4 K44A mutant strains. By extrapolation, a missegregation frequency of 8% for a single chromosome means that <26% of the mutant cells would be able to segregate all 16 chromosomes properly, consistent with the strong growth defects observed in these mutant strains. There were minor defects in the

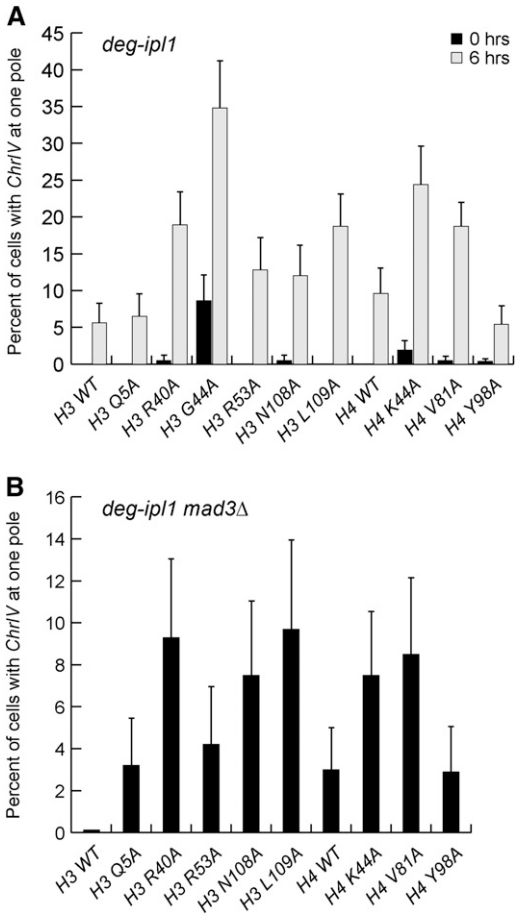

Figure 3 Analysis of sister-chromatid segregation in the histone mutant strains. (A) Asynchronous cultures of *deg-ipl1* strains (SBY9837–SBY9847) were grown in doxycycline for 0 or 6 hr, and *ChrIV* segregation was monitored in anaphase cells that had DNA masses at opposite poles. (B) *deg-ipl1 mad3*Δ strains containing WT H3 and H4 or the mutations indicated (SBY9848–SBY9858) were released from G1 in the presence of doxycycline. *ChrIV* segregation was monitored in anaphase cells with DNA masses at opposite poles.

H3 Q5A and H3 R53A mutant strains and no observable defect in the H4 Y98A strain. Whereas the H4 V81A strain appeared to have a missegregation defect, >4% of G1-arrested cells exhibited two GFP foci, indicative of aneuploidy, as compared to <1.3% in all other strains. *H3 G44A* mutant cells were not quantified in this experiment because >5% of cells exhibited two GFP foci in the G1 arrest, indicating preexisting aneuploidy that makes accurate quantification impossible.

Expression of segregation genes is not significantly altered in the histone mutants

To determine whether the segregation defects may be due to altered transcription of segregation genes, we performed DNA microarray expression analysis on each mutant. RNA was prepared from asynchronous cultures of WT or histone mutant strains (without *deg-ipl1*). The complementary RNA was then labeled and hybridized to 70-mer oligonucleotide microarrays. Each mutant was analyzed for gene expression changes >1.7-fold up or down and with a *P*-value <0.01. We analyzed the list (Table S2) for genes known to be involved in kinetochore function or chromosome segregation and did not find any mutant that significantly altered any chromosome segregation genes. We note that H3 G44A, H4 K44A, and H4 V81A exhibit aneuploidy based on their gene expression profile, consistent with their segregation defects. Together, the microarray data suggest that the segregation defects in the histone mutants are not due to the altered transcription of one or more genes required for kinetochore function.

Cse4 localization to centromeres is normal in the histone mutants

Because the kinetochore assembles on a specialized chromatin structure, we reasoned that the histone mutants might alter the chromatin at and/or around centromeres, thus disrupting chromosome segregation. Yeast centromeres contain a single well-positioned nucleosome that contains the specialized histone H3 variant Cse4 (Stoler *et al.* 1995; Meluh *et al.* 1998; Furuyama and Biggins 2007; Krassovsky *et al.* 2012). We therefore tested whether total Cse4 levels are altered by any of the histone mutants by performing quantitative immunoblotting on crude lysates from WT and histone mutant strains with antibodies against Cse4. We compared the ratio of Cse4 to Pgk1, a loading control, and found that Cse4 levels are close to WT (±10%) in most of the strains. However, Cse4 levels were decreased by 13% in the H3 L109A mutant and 29% in the H4 V81A mutants and increased by 17% in the H3 R53A mutant strain (Figure 4A). The microarray data did not reveal any significant change in the transcription of *CSE4* in these mutants, indicating that the lower protein levels are likely due to a post-transcriptional effect. Cse4 levels are tightly regulated by proteolysis, so the H4 V81A mutant may alter the function or accessibility of the ubiquitin ligase that regulates Cse4 (Collins *et al.* 2004; Hewawasam *et al.* 2010; Ranjitkar *et al.* 2010). Although it is unclear how H3 mutants would alter Cse4 levels, they may affect the ability of Cse4 to incorporate into euchromatin, which could affect the accessibility of Psh1 to degrade Cse4.

We next asked whether Cse4 incorporation at the centromere was affected in any of the histone mutant strains. Although most of the mutants that we identified are in H3, changes in the nucleosomes surrounding the centromere could lead to changes in Cse4 incorporation at centromeres. In addition, it was recently reported that H3 also localizes to centromeres (Lochmann and Ivanov 2012), although the resolution of the assay used cannot discriminate between localization at the core centromere and surrounding nucleosomes. To analyze Cse4 localization at centromeres, we performed ChIP on the *deg-ipl1* histone mutant strains grown in doxycycline for 6 hr. The cells contained a nonessential minichromosome so that we could analyze Cse4 in the context of a plasmid in addition to the endogenous centromere (Akiyoshi *et al.* 2009). Cse4 was

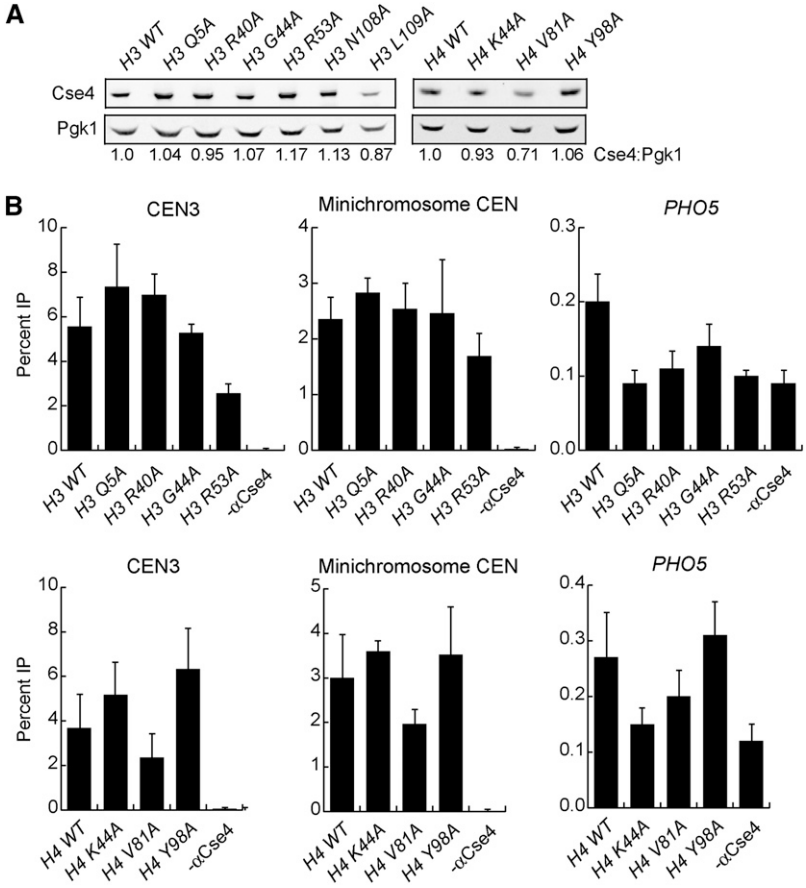

Figure 4 Analysis of Cse4 levels and localization to the centromere in the H3 and H4 mutants. (A) The indicated *deg-ipl1* histone mutant strains (SBY10182–10192) were grown in doxycycline for 6 hr, and crude lysates were immunoblotted with anti-Cse4 and anti-Pgk1 antibodies for quantitative analysis. A representative immunoblot is shown, and the mean quantified Cse4-to-Pgk1 ratio relative to the corresponding WT parent is reported under each lane. (B) Cse4 ChIP was performed on *deg-ipl1* H3 (top) and H4 (bottom) mutant strains (SBY10182–10192) containing centromeric minichromosomes grown in doxycycline for 6 hr. Quantitative real-time PCR was carried out using oligos specific to endogenous CEN3, the minichromosome CEN, and a control locus (*PHO5*).

immunoprecipitated and the amount of DNA bound to Cse4 was analyzed by standard PCR with primers to the centromere. There was no obvious change in any of the strains (data not shown), so we analyzed a subset of them using quantitative real-time PCR with primers to the centromeres or a control locus, *PHO5* (Figure 4B). This revealed a slight decrease in Cse4 bound to the centromere in the H4 V81A mutant that had lower Cse4 levels in the lysate. There was also a slight decrease in the level of Cse4 at the endogenous centromere in the H3 R53A mutant that had higher levels of total Cse4, although this was not apparent on the minichromosome. We have not previously detected changes in centromere-bound Cse4 when the gene is overexpressed (Collins *et al.* 2004), so this result is likely related to changes in the chromatin due to the H3 mutation rather than the altered Cse4 levels. The remaining mutants showed no significant differences in the level of Cse4 at either the endogenous or minichromosome centromere when compared to WT. Together, these data demonstrate that the histone mutants do not significantly alter Cse4 localization to the centromere.

Kinetochore stability is altered in the histone mutant strains

We next asked whether overall kinetochore integrity is normal in the mutants by purifying centromeric minichromosomes (Akiyoshi *et al.* 2009). In contrast to ChIP techniques that require a cross-linking step prior to immunoprecipitation, the minichromosome purification technique isolates native material and can therefore reveal subtle changes in kinetochore stability. A centromeric minichromosome containing *LacO* sequences was introduced into each *deg-ipl1* histone mutant that also expressed *LacI-Flag*, and the cells were grown asynchronously in doxycycline for 6 hr. We did not detect major alterations in the total protein levels of representative core kinetochore proteins in the lysates prepared from each histone mutant strain other than a slight reduction in Ndc10 levels in the H3 L109A mutant strain (Figure 5A). We therefore immunoprecipitated *Lac*I-Flag and analyzed the purified minichromosome samples for the levels of copurifying kinetochore proteins. The Ndc10 protein is a component of the CBF3 complex that binds directly to the CDEIII element of the yeast centromere (Lechner and Carbon 1991). Because Ndc10 binding is unlikely to be affected by changes in neighboring nucleosomes (Cho and Harrison 2012), we compared the relative levels of representative components spanning the inner (Mif2, Ctf19, and Cse4) and outer kinetochore (Spc105 and Ndc80) to Ndc10 levels (Figure 5B). In the H3 Q5A, H3 N108A, and H4 Y98A histone mutant strains, the levels of kinetochore proteins bound to minichromosomes were similar to WT. However, in the H3 G44A mutant, there was a decrease in all components, consistent with previous

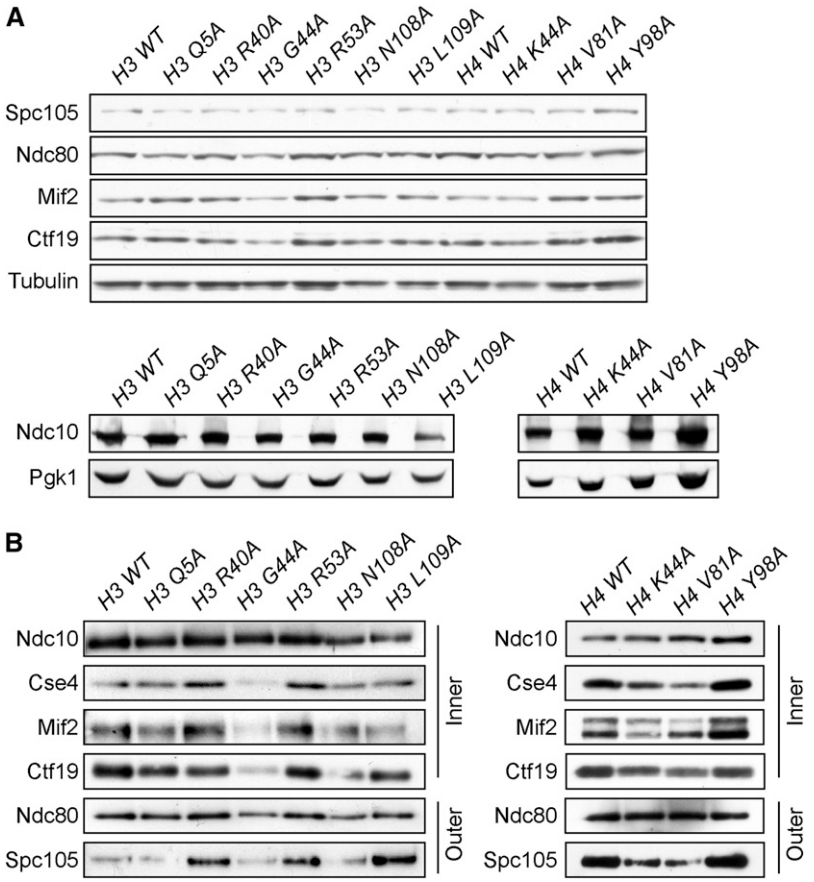

Figure 5 Analysis of kinetochore composition on minichromosomes purified from H3 and H4 mutant strains. (A) The indicated *deg-ipl1* histone mutant strains (SBY10182–10192) were grown asynchronously in doxycycline for 6 hr and immunoblotted with antibodies against the indicated kinetochore proteins. Tubulin or Pgk1 are shown as loading controls. (B) Centromeric minichromosomes were immunoprecipitated from *deg-ipl1* H3 (left) and H4 (right) mutant strains (SBY10182–10192) grown in doxycycline for 6 hr. The purifications were immunoblotted for the indicated outer kinetochore proteins (Spc105, Ndc80) and inner (Mif2, Ctf19, Cse4) kinetochore proteins. Ndc10 directly binds to the centromere and was used as a loading control.

work that showed that this residue contributes to segregation (Luo *et al.* 2010). The H4 K44A and H4 V81A mutants appeared to copurify somewhat lower levels of the inner kinetochore components Cse4, Mif2, and Ctf19, revealing an overall defect in inner kinetochore stability. Because the levels of Cse4 at the centromere were not significantly different from WT in these mutants when assayed by ChIP (see Figure 4B), our data are consistent with the possibility that there is a subtle defect in kinetochore stability that is revealed during the purification of the minichromosome. Consistent with this, the Spc105 outer kinetochore protein was also reduced in these two H4 mutants. We note that, although H4 K44 is a key residue in Set2 methylation of H3 K36 (Du *et al.* 2008), the latter residue was not identified in our screens. Surprisingly, the H3 R40A, H3 R53A, and H3 L109A mutants appeared to have a stronger association of one or more kinetochore proteins relative to Ndc10 than WT. While the underlying mechanism is not clear, it was recently reported that a deletion of the Cnn1 kinetochore protein leads to a more robust association between outer kinetochore proteins (Bock *et al.* 2012). Cnn1 is the budding yeast ortholog of the chromatin-associated Cenp-T protein (Nishino *et al.* 2012; Schleiffer *et al.* 2012), raising the possibility that its function is altered in these histone mutants. Regardless of the mechanism, the kinetochore appears to be more robust to purification in the presence of these mutations.

High-copy SGO1 can alleviate defects in some histone mutant strains

Pericentromeric chromatin recruits the Sgo1 protein to facilitate biorientation and the tension checkpoint. Because both Ipl1 and Sgo1 have roles in kinetochore biorientation and the tension checkpoint (Biggins *et al.* 1999; Biggins and Murray 2001; Indjeian *et al.* 2005; Indjeian and Murray 2007), we considered the possibility that the histone mutants have defects in Sgo1 function. Consistent with this, we identified the H3 G44 residue near the nucleosome entry/exit site that is required for Sgo1 localization to pericentromeric chromatin in our screen (Luo *et al.* 2010). In addition, we also identified two other residues near the nucleosome entry exit site (H3 R40 and H4 K44) as well as two buried residues that could affect this region (H3 N108 and H3 L109). High-copy *SGO1* can suppress the mitotic defects in an H3 G44S mutant (Luo *et al.* 2010), so we tested whether *SGO1* overexpression has an effect on the histone mutants that we identified. We analyzed the growth of *deg-ipl1* histone mutant strains containing a high-copy *SGO1* plasmid in the presence and absence of doxycycline (Figure 6A). We found that H3 R40A, H3 G44A, H3 N108A, H3 L109A, and H4 K44A were all suppressed to varying degrees while the growth of the other mutants was not affected. These data strongly suggest that Sgo1 function is compromised in these histone mutants and may be the underlying mechanism that leads to defects in segregation and biorientation.

Strikingly, all of these residues are close to the nucleosome/entry exit site, suggesting that we have further defined structural constraints of the nucleosome required for Sgo1 localization and/or function at centromeres.

Discussion

In sum, we utilized an H3 and H4 mutant library to identify residues that ensure the fidelity of chromosome segregation. Although many screens for histone mutations that affect genomic stability have been reported (Smith *et al.* 1996; Hyland *et al.* 2005; Matsubara *et al.* 2007; Dai *et al.* 2008; Sakamoto *et al.* 2009; Kawashima *et al.* 2011; Yu *et al.* 2011), none have been specifically directed at measuring chromosome segregation frequencies or sensitivity to Ipl1/Aurora downregulation. While this work was in progress, Kawashima *et al*. (2011) reported a systematic screen of all histone mutants for sensitivity to the microtubule-depolymerizing agents benomyl and thiabendazole. There was little overlap of mutants identified in their study with those identified here, with the exception of H3 G44A and H4 Y98A. The lack of overlap could potentially be due to off-target effects of the drugs.

Our work identified the H3 residues Q5, R40, G44, R53, N108, and L109 and the H4 residues K44, V81, and Y98 as important for segregation and biorientation. While it is unclear how all of the residues that we identified contribute to these processes, five of the mutants reside near the nucleosome entry/exit site and can be suppressed by increasing the dosage of *SGO1*, consistent with the Sgo1-binding site spanning this region of the nucleosome. An attractive hypothesis is that the DNA at the entry/exit site of the nucleosome may come under tension when kinetochores biorient, thus signaling to the cell that the kinetochores have achieved biorientation. Consistent with this, tension-dependent changes in budding yeast pericentromeric chromatin structure have been observed by microscopy (Haase *et al.* 2012; Verdaasdonk *et al.* 2012). The localization of Sgo1 to this region may therefore be coupled to its ability to trigger the spindle checkpoint when the pericentromeric chromatin is not under tension. Sgo1 and Bub1 modulate pericentromeric chromatin structure in response to microtubule dynamics (Haase *et al.* 2012), so it is possible that the histone mutations that we have identified alter a specific structural property associated with pericentromeres. We attempted to analyze chromatin structure in the pericentromere region in the absence of tension and Sgo1, but the resolution of the assay that we used was not sensitive enough to detect any changes (data not shown). In addition, we were not able to detect significant changes in Sgo1 localization to pericentromeres by ChIP (data not shown). An important future direction will be to determine how the interaction between Sgo1 and nucleosomes mechanistically contributes to biorientation. It will also be important to understand how the other histone mutants that we identified contribute to chromosome segregation and thus maintain genomic stability. It was recently shown that histones in the pericentromere are turned over at a higher rate than the arms, so one possibility is that the mutants that we identified alter histone dynamics within the pericentromere (Verdaasdonk *et al.* 2012). Our work provides a foundation for further mechanistic studies aimed at understanding the role of centromeric and pericentromeric chromatin in chromosome segregation.

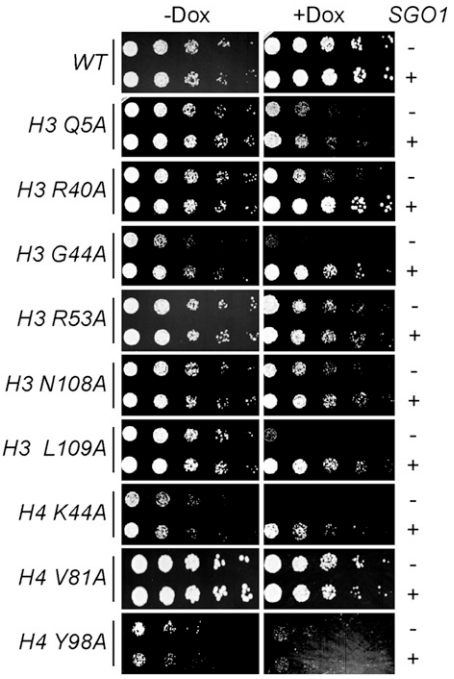

Figure 6 Analysis of *SGO1* overexpression in the *deg-ipl1* histone mutant strains. Fivefold serial dilutions of *deg-ipl1* histone mutant strains containing a control (−) or high-copy *SGO1* plasmid (+) (SBY9870, SBY9871, SBY9874 SBY9875, and SBY10284–SBY10297) were analyzed for growth in the presence and absence of doxycycline.

Acknowledgments

We thank Shawna Miles and Laura Lee for help with the FACS analysis; Jairo Rodriguez, Toshi Tsukiyama, and the Biggins lab for helpful discussions and advice; Minhao Kuo and Arshad Desai for reagents; and Toshi Tsukiyama for comments on the manuscript. T.M.N. was supported in part by Public Health Service, National Research Service Award T32 GM07270 from the National Institute of General Medical Sciences. T.L.L. and F.C.P.H. are supported by The Netherlands Organization of Scientific Research. This work was also supported by National Institutes of Health grant GM078079 to S.B. and U54RR020839 to J.D.B.

Literature Cited

Akiyoshi, B., C. R. Nelson, J. A. Ranish, and S. Biggins, 2009 Quantitative proteomic analysis of purified yeast kinetochores identifies a PP1 regulatory subunit. Genes Dev. 23: 2887–2899.

Akiyoshi, B., K. K. Sarangapani, A. F. Powers, C. R. Nelson, S. L. Reichow *et al.*, 2010 Tension directly stabilizes reconstituted kinetochore-microtubule attachments. Nature 468: 576–579.

Baker, S. P., J. Phillips, S. Anderson, Q. Qiu, J. Shabanowitz *et al.*, 2010 Histone H3 Thr 45 phosphorylation is a replication-associated post-translational modification in *S. cerevisiae*. Nat. Cell Biol. 12: 294–298.

Biggins, S., and A. W. Murray, 2001 The budding yeast protein kinase Ipl1/Aurora allows the absence of tension to activate the spindle checkpoint. Genes Dev. 15: 3118–3129.

Biggins, S., F. F. Severin, N. Bhalla, I. Sassoon, A. A. Hyman *et al.*, 1999 The conserved protein kinase Ipl1 regulates microtubule binding to kinetochores in budding yeast. Genes Dev. 13: 532–544.

Blat, Y., and N. Kleckner, 1999 Cohesins bind to preferential sites along yeast chromosome III, with differential regulation along arms *vs.* the centric region. Cell 98: 249–259.

Blower, M. D., B. A. Sullivan, and G. H. Karpen, 2002 Conserved organization of centromeric chromatin in flies and humans. Dev. Cell 2: 319–330.

Bock, L. J., C. Pagliuca, N. Kobayashi, R. A. Grove, Y. Oku *et al.*, 2012 Cnn1 inhibits the interactions between the KMN complexes of the yeast kinetochore. Nat. Cell Biol. 14: 614–624.

Brachmann, C. B., A. Davies, G. J. Cost, E. Caputo, J. Li *et al.*, 1998 Designer deletion strains derived from *Saccharomyces cerevisiae* S288C: a useful set of strains and plasmids for PCR-mediated gene disruption and other applications. Yeast 14: 115–132.

Cam, H. P., T. Sugiyama, E. S. Chen, X. Chen, P. C. FitzGerald *et al.*, 2005 Comprehensive analysis of heterochromatin- and RNAi-mediated epigenetic control of the fission yeast genome. Nat. Genet. 37: 809–819.

Chambers, A. L., G. Ormerod, S. C. Durley, T. L. Sing, G. W. Brown *et al.*, 2012 The INO80 chromatin remodeling complex prevents polyploidy and maintains normal chromatin structure at centromeres. Genes Dev. 26: 2590–2603.

Cho, U. S., and S. C. Harrison, 2012 Ndc10 is a platform for inner kinetochore assembly in budding yeast. Nat. Struct. Mol. Biol. 19: 48–55.

Collins, K. A., S. Furuyama, and S. Biggins, 2004 Proteolysis contributes to the exclusive centromere localization of the yeast Cse4/CENP-A histone H3 variant. Curr. Biol. 14: 1968–1972.

Collins, K. A., A. R. Castillo, S. Y. Tatsutani, and S. Biggins, 2005 De novo kinetochore assembly requires the centromeric histone H3 variant. Mol. Biol. Cell 16: 5649–5660.

Compton, D. A., 2011 Mechanisms of aneuploidy. Curr. Opin. Cell Biol. 23: 109–113.

Cooke, C. A., M. M. Heck, and W. C. Earnshaw, 1987 The inner centromere protein (INCENP) antigens: movement from inner centromere to midbody during mitosis. J. Cell Biol. 105: 2053–2067.

Dai, J., B. A. Sullivan, and J. M. Higgins, 2006 Regulation of mitotic chromosome cohesion by Haspin and Aurora B. Dev. Cell 11: 741–750.

Dai, J., E. M. Hyland, D. S. Yuan, H. Huang, J. S. Bader *et al.*, 2008 Probing nucleosome function: a highly versatile library of synthetic histone H3 and H4 mutants. Cell 134: 1066–1078.

Du, H. N., I. M. Fingerman, and S. D. Briggs, 2008 Histone H3 K36 methylation is mediated by a trans-histone methylation pathway involving an interaction between Set2 and histone H4. Genes Dev. 22: 2786–2798.

Eckert, C. A., D. J. Gravdahl, and P. C. Megee, 2007 The enhancement of pericentromeric cohesin association by conserved kinetochore components promotes high-fidelity chromosome segregation and is sensitive to microtubule-based tension. Genes Dev. 21: 278–291.

Fuller, B. G., M. A. Lampson, E. A. Foley, S. Rosasco-Nitcher, K. V. Le *et al.*, 2008 Midzone activation of aurora B in anaphase produces an intracellular phosphorylation gradient. Nature 453: 1132–1136.

Furuyama, S., and S. Biggins, 2007 Centromere identity is specified by a single centromeric nucleosome in budding yeast. Proc. Natl. Acad. Sci. USA 104: 14706–14711.

Gietz, R. D., and A. Sugino, 1988 New yeast-*Escherichia coli* shuttle vectors constructed with in vitro mutagenized yeast genes lacking six-base pair restriction sites. Gene 74: 527–534.

Gutierrez-Caballero, C., L. R. Cebollero, and A. M. Pendas, 2012 Shugoshins: from protectors of cohesion to versatile adaptors at the centromere. Trends Genet. 28: 351–360.

Haase, J., A. Stephens, J. Verdaasdonk, E. Yeh, and K. Bloom, 2012 Bub1 kinase and Sgo1 modulate pericentric chromatin in response to altered microtubule dynamics. Curr. Biol. 22: 471–481.

Henikoff, S., and J. G. Henikoff, 2012 "Point" centromeres of *Saccharomyces* harbor single centromere-specific nucleosomes. Genetics 190: 1575–1577.

Hewawasam, G., M. Shivaraju, M. Mattingly, S. Venkatesh, S. Martin-Brown *et al.*, 2010 Psh1 is an E3 ubiquitin ligase that targets the centromeric histone variant Cse4. Mol. Cell 40: 444–454.

Hieter, P., C. Mann, M. Snyder, and R. W. Davis, 1985 Mitotic stability of yeast chromosomes: a colony colour assay that measures nondisjunction and chromosome loss. Cell 40: 381–392.

Hyland, E. M., M. S. Cosgrove, H. Molina, D. Wang, A. Pandey *et al.*, 2005 Insights into the role of histone H3 and histone H4 core modifiable residues in *Saccharomyces cerevisiae*. Mol. Cell. Biol. 25: 10060–10070.

Indjeian, V. B., and A. W. Murray, 2007 Budding yeast mitotic chromosomes have an intrinsic bias to biorient on the spindle. Curr. Biol. 17: 1837–1846.

Indjeian, V. B., B. M. Stern, and A. W. Murray, 2005 The centromeric protein Sgo1 is required to sense lack of tension on mitotic chromosomes. Science 307: 130–133.

Kawashima, S. A., T. Tsukahara, M. Langegger, S. Hauf, T. S. Kitajima *et al.*, 2007 Shugoshin enables tension-generating attachment of kinetochores by loading Aurora to centromeres. Genes Dev. 21: 420–435.

Kawashima, S. A., Y. Yamagishi, T. Honda, K. Ishiguro, and Y. Watanabe, 2010 Phosphorylation of H2A by Bub1 prevents chromosomal instability through localizing shugoshin. Science 327: 172–177.

Kawashima, S., Y. Nakabayashi, K. Matsubara, N. Sano, T. Enomoto *et al.*, 2011 Global analysis of core histones reveals nucleosomal surfaces required for chromosome bi-orientation. EMBO J. 30: 3353–3367.

Kelly, A. E., C. Ghenoiu, J. Z. Xue, C. Zierhut, H. Kimura *et al.*, 2010 Survivin reads phosphorylated histone H3 threonine 3 to activate the mitotic kinase Aurora B. Science 330: 235–239.

Kiburz, B. M., D. B. Reynolds, P. C. Megee, A. L. Marston, B. H. Lee *et al.*, 2005 The core centromere and Sgo1 establish a 50-kb cohesin-protected domain around centromeres during meiosis I. Genes Dev. 19: 3017–3030.

Kiburz, B. M., A. Amon, and A. L. Marston, 2008 Shugoshin promotes sister kinetochore biorientation in *Saccharomyces cerevisiae*. Mol. Biol. Cell 19: 1199–1209.

Krassovsky, K., J. G. Henikoff, and S. Henikoff, 2012 Tripartite organization of centromeric chromatin in budding yeast. Proc. Natl. Acad. Sci. USA 109: 243–248.

Lampson, M. A., and I. M. Cheeseman, 2011 Sensing centromere tension: Aurora B and the regulation of kinetochore function. Trends Cell Biol. 21: 133–140.

Lawrimore, J., K. S. Bloom, and E. D. Salmon, 2011 Point centromeres contain more than a single centromere-specific Cse4 (CENP-A) nucleosome. J. Cell Biol. 195: 573–582.

Lechner, J., and J. Carbon, 1991 A 240 kd multisubunit protein complex, CBF3, is a major component of the budding yeast centromere. Cell 64: 717–725.

Liu, D., and M. A. Lampson, 2009 Regulation of kinetochore-microtubule attachments by Aurora B kinase. Biochem. Soc. Trans. 37: 976–980.

Liu, D., G. Vader, M. J. Vromans, M. A. Lampson, and S. M. Lens, 2009 Sensing chromosome bi-orientation by spatial separation of aurora B kinase from kinetochore substrates. Science 323: 1350–1353.

Lochmann, B., and D. Ivanov, 2012 Histone H3 localizes to the centromeric DNA in budding yeast. PLoS Genet. 8: e1002739.

Luger, K., A. W. Mader, R. K. Richmond, D. F. Sargent, and T. J. Richmond, 1997 Crystal structure of the nucleosome core particle at 2.8 A resolution. Nature 389: 251–260.

Luo, J., X. Xu, H. Hall, E. M. Hyland, J. D. Boeke *et al.*, 2010 Histone H3 exerts a key function in mitotic checkpoint control. Mol. Cell. Biol. 30: 537–549.

Maddox, P. S., K. D. Corbett, and A. Desai, 2012 Structure, assembly and reading of centromeric chromatin. Curr. Opin. Genet. Dev. 22: 139–147.

Maresca, T. J., and E. D. Salmon, 2010 Welcome to a new kind of tension: translating kinetochore mechanics into a wait-anaphase signal. J. Cell Sci. 123: 825–835.

Margaritis, T., P. Lijnzaad, D. van Leenen, D. Bouwmeester, P. Kemmeren *et al.*, 2009 Adaptable gene-specific dye bias correction for two-channel DNA microarrays. Mol. Syst. Biol. 5: 266.

Matsubara, K., N. Sano, T. Umehara, and M. Horikoshi, 2007 Global analysis of functional surfaces of core histones with comprehensive point mutants. Genes Cells 12: 13–33.

Meluh, P. B., P. Yang, L. Glowczewski, D. Koshland, and M. M. Smith, 1998 Cse4p is a component of the core centromere of *Saccharomyces cerevisiae*. Cell 94: 607–613.

Minshull, J., A. Straight, A. Rudner, A. Dernburg, A. Belmont *et al.*, 1996 Protein phosphatase 2A regulates MPF activity and sister chromatid cohesion in budding yeast. Curr. Biol. 6: 1609–1620.

Musacchio, A., 2011 Spindle assembly checkpoint: the third decade. Philos. Trans. R. Soc. Lond. B Biol. Sci. 366: 3595–3604.

Nasmyth, K., 2011 Cohesin: A catenase with separate entry and exit gates? Nat. Cell Biol. 13: 1170–1177.

Nezi, L., and A. Musacchio, 2009 Sister chromatid tension and the spindle assembly checkpoint. Curr. Opin. Cell Biol. 21: 785–795.

Ng, T. M., W. G. Waples, B. D. Lavoie, and S. Biggins, 2009 Pericentromeric sister chromatid cohesion promotes kinetochore biorientation. Mol. Biol. Cell 20: 3818–3827.

Nishino, T., K. Takeuchi, K. E. Gascoigne, A. Suzuki, T. Hori *et al.*, 2012 CENP-T-W-S-X forms a unique centromeric chromatin structure with a histone-like fold. Cell 148: 487–501.

Oliveira, R. A., and K. Nasmyth, 2010 Getting through anaphase: splitting the sisters and beyond. Biochem. Soc. Trans. 38: 1639–1644.

Pinsky, B. A., S. Y. Tatsutani, K. A. Collins, and S. Biggins, 2003 An Mtw1 complex promotes kinetochore biorientation that is monitored by the Ipl1/Aurora protein kinase. Dev. Cell 5: 735–745.

Ranjitkar, P., M. O. Press, X. Yi, R. Baker, M. J. MacCoss *et al.*, 2010 An E3 ubiquitin ligase prevents ectopic localization of the centromeric histone H3 variant via the centromere targeting domain. Mol. Cell 40: 455–464.

Resnick, T. D., D. L. Satinover, F. MacIsaac, P. T. Stukenberg, W. C. Earnshaw *et al.*, 2006 INCENP and Aurora B promote meiotic sister chromatid cohesion through localization of the Shugoshin MEI-S332 in *Drosophila*. Dev. Cell 11: 57–68.

Rose, M. D., F. Winston, and P. Heiter, 1990 *Methods in Yeast Genetics*. Cold Spring Harbor Laboratory Press, Cold Spring Harbor, NY.

Sakamoto, M., S. Noguchi, S. Kawashima, Y. Okada, T. Enomoto *et al.*, 2009 Global analysis of mutual interaction surfaces of nucleosomes with comprehensive point mutants. Genes Cells 14: 1271–1330.

Schleiffer, A., M. Maier, G. Litos, F. Lampert, P. Hornung *et al.*, 2012 CENP-T proteins are conserved centromere receptors of the Ndc80 complex. Nat. Cell Biol. 14: 604–613.

Sherman, F., G. Fink, and C. Lawrence, 1974 *Methods in Yeast Genetics*. Cold Spring Harbor Laboratory Press, Cold Spring Harbor, NY.

Sikorski, R. S., and P. Hieter, 1989 A system of shuttle vectors and yeast host strains designed for efficient manipulation of DNA in *Saccharomyces cerevisiae*. Genetics 122: 19–27.

Smith, M. M., P. Yang, M. S. Santisteban, P. W. Boone, A. T. Goldstein *et al.*, 1996 A novel histone H4 mutant defective in nuclear division and mitotic chromosome transmission. Mol. Cell. Biol. 16: 1017–1026.

Stellfox, M. E., A. O. Bailey, and D. R. Foltz, 2012 Putting CENP-A in its place. Cell. Mol. Life Sci.

Stoler, S., K. C. Keith, K. E. Curnick, and M. Fitzgerald-Hayes, 1995 A mutation in *CSE4*, an essential gene encoding a novel chromatin-associated protein in yeast, causes chromosome nondisjunction and cell cycle arrest at mitosis. Genes Dev. 9: 573–586.

Storchova, Z., J. S. Becker, N. Talarek, S. Kogelsberger, and D. Pellman, 2011 Bub1, Sgo1, and Mps1 mediate a distinct pathway for chromosome biorientation in budding yeast. Mol. Biol. Cell 22: 1473–1485.

Straight, A. F., A. S. Belmont, C. C. Robinett, and A. W. Murray, 1996 GFP tagging of budding yeast chromosomes reveals that protein-protein interactions can mediate sister chromatid cohesion. Curr. Biol. 6: 1599–1608.

Tanaka, T., M. P. Cosma, K. Wirth, and K. Nasmyth, 1999 Identification of cohesin association sites at centromeres and along chromosome arms. Cell 98: 847–858.

Tanaka, T. U., N. Rachidi, C. Janke, G. Pereira, M. Galova *et al.*, 2002 Evidence that the Ipl1-Sli15 (Aurora kinase-INCENP) complex promotes chromosome bi-orientation by altering kinetochore-spindle pole connections. Cell 108: 317–329.

Valente, L. P., M. C. Silva, and L. E. Jansen, 2012 Temporal control of epigenetic centromere specification. Chromosome Res. 20: 481–492.

van de Peppel, J., P. Kemmeren, H. van Bakel, M. Radonjic, D. van Leenen *et al.*, 2003 Monitoring global messenger RNA changes in externally controlled microarray experiments. EMBO Rep. 4: 387–393.

Vanoosthuyse, V., S. Prykhozhij, and K. G. Hardwick, 2007 Shugoshin 2 regulates localization of the chromosomal passenger proteins in fission yeast mitosis. Mol. Biol. Cell 18: 1657–1669.

Vaur, S., F. Cubizolles, G. Plane, S. Genier, P. K. Rabitsch *et al.*, 2005 Control of Shugoshin function during fission-yeast meiosis. Curr. Biol. 15: 2263–2270.

Verdaasdonk, J. S., R. Gardner, A. D. Stephens, E. Yeh, and K. Bloom, 2012 Tension-dependent nucleosome remodeling at the pericentromere in yeast. Mol. Biol. Cell 23: 2560–2570.

Wang, F., J. Dai, J. R. Daum, E. Niedzialkowska, B. Banerjee *et al.*, 2010 Histone H3 Thr-3 phosphorylation by Haspin positions Aurora B at centromeres in mitosis. Science 330: 231–235.

Watanabe, Y., 2005 Shugoshin: guardian spirit at the centromere. Curr. Opin. Cell Biol. 17: 590–595.

Williams, B. R., and A. Amon, 2009 Aneuploidy: Cancer's fatal flaw? Cancer Res. 69: 5289–5291.

Yamagishi, Y., T. Honda, Y. Tanno, and Y. Watanabe, 2010 Two histone marks establish the inner centromere and chromosome bi-orientation. Science 330: 239–243.

Yeh, E., J. Haase, L. V. Paliulis, A. Joglekar, L. Bond *et al.*, 2008 Pericentric chromatin is organized into an intramolecular loop in mitosis. Curr. Biol. 18: 81–90.

Yu, Y., M. Srinivasan, S. Nakanishi, J. Leatherwood, A. Shilatifard *et al.*, 2011 A conserved patch near the C terminus of histone H4 is required for genome stability in budding yeast. Mol Cell Biol 31: 2311–2325.

Communicating editor: N. M. Hollingsworth

GENETICS

Supporting Information
http://www.genetics.org/lookup/suppl/doi:10.1534/genetics.113.152082/-/DC1

Kinetochore Function and Chromosome Segregation Rely on Critical Residues in Histones H3 and H4 in Budding Yeast

Tessie M. Ng, Tineke L. Lenstra, Nicole Duggan, Shuangying Jiang, Steven Ceto, Frank C. P. Holstege, Junbiao Dai, Jef D. Boeke, and Sue Biggins

DOI: 10.1534/genetics.113.152082

Table S1 Viability of histone mutants in various strain backgrounds. Mutants that were not tested (-) because viable transformants could not be generated in the indicated strains.

Histone residue	S288c/ GRF167*	W303 *deg-IPL1*
H3 Y41	viable	-
H3 K42	-	viable
H3 T45	-	viable
H3 L48	-	viable
H3 I51	-	viable
H3 R52	-	viable
H3 F54	-	viable
H3 I62	-	-
H3 F67	-	viable
H3 Q68	viable	-
H3 F78	viable	-
H3 F84	-	viable
H3 I89	viable	-
H3 Q93	-	viable
H3 E94	viable	-
H3 S95	-	viable
H3 E97	-	-
H3 L103	viable	-
H3 T107	-	viable
H3 N108	-	viable
H3 I112	viable	-
H3 H113	-	-
H3 K115	-	viable
H3 R116	-	-
H3 T118	-	-
H3 I119	viable	-
H3 Q120	-	viable
H3 D123	-	-
H3 L126	-	viable
H3 L130	-	viable
H4 G9	viable	-
H4 I34	-	viable
H4 R39	-	-
H4 R40	-	-
H4 K44	-	viable
H4 R45	-	-
H4 Y51	-	viable
H4 F61	-	viable
H4 L62	viable	-
H4 S69	-	viable
H4 Y72	-	-
H4 T73	-	viable
H4 A76	-	-
H4 R78	-	-
H4 T80	-	viable
H4 S83	-	viable
H4 L84	-	-
H4 D85	-	viable
H4 Y88	-	viable
H4 L90	-	viable
H4 K91	-	-
H4 L97	viable	-
H4 Y98	-	viable

*Lethality (-) in S288C and GRF167 was previously reported (Dai *et al.*, 2008).

LITERATURE CITED

Dai, J., Hyland, E.M., Yuan, D.S., Huang, H., Bader, J.S., and Boeke, J.D. (2008). Probing nucleosome function: a highly versatile library of synthetic histone H3 and H4 mutants. Cell *134*, 1066-1078.

Table S2 The expression of segregation genes is not significantly altered in the histone mutants. Significantly up- and downregulated genes (fold change > 1.7 and $p < 0.01$) of different histone mutants as determined by microarray analysis. The up- and downregulated genes in this list do not overlap with genes involved in kinetochore function or chromosome segregation.

Table S2 is available for download at http://www.genetics.org/lookup/suppl/doi:10.1534/genetics.113.152082/-/DC1.

Table S3 Yeast strains used in this study.

Strain	Genotype
SBY9119	*MATa ura3-1 leu2-3,112 his3-11:pCUP1GFP12-LacI12:HIS trp1-1:lacO:TRP1 can1-100 ade2-1:7-tetOp-Ub-R-IPL1:ADE2 BAR1 ipl1ΔKAN hht1-hhf1ΔHYG*
SBY9120	*MATa ura3-1 leu2-3,112 his3-11:pCUP1GFP12-LacI12:HIS trp1-1:lacO:TRP1 can1-100 ade2-1:7-tetOp-Ub-R-IPL1:ADE2 BAR1 ipl1ΔKAN hht1-hhf1ΔHYG ura3ΔNAT*
JDY168	*MATa, ura3-1, leu2-3,112, his3-112, trp1-1, can1-100, ade2-1, bar1-1, SUP11 CFIII(CEN3, YPH983):HIS3 hht1-hhf1::NatMX4*
JDY176	*MATa, ura3Δ0, leu2-3,11, his3-11, trp1-1, can1-100, ade2-1, bar1-1, SUP11 CFIII(CEN3, YPH983):HIS3 hht1-hhf1::NatMX4*

All subsequent H3 strains are derivatives of SBY9120 and H4 strains of SBY9119.

Strain	Histone mutation
SBY9621	*H3 A1S*
SBY9622	*H3 R2A*
SBY9623	*H3 T3A*
SBY9624	*H3 K4A*
SBY9625	*H3 Q5A*
SBY9626	*H3 T6A*
SBY9627	*H3 A7S*
SBY9628	*H3 R8A*
SBY9629	*H3 K9A*
SBY9630	*H3 S10A*
SBY9631	*H3 T11A*
SBY9632	*H3 G12A*
SBY9633	*H3 G13A*
SBY9634	*H3 K14A*
SBY9635	*H3 A15S*
SBY9636	*H3 P16A*
SBY9637	*H3 R17A*
SBY9638	*H3 K18A*
SBY9639	*H3 Q19A*
SBY9640	*H3 L20A*
SBY9641	*H3 A21S*
SBY9642	*H3 S22A*
SBY9643	*H3 K23A*
SBY9644	*H3 A24S*
SBY9645	*H3 A25S*
SBY9646	*H3 R26A*
SBY9647	*H3 K27A*
SBY9648	*H3 S28A*
SBY9649	*H3 A29S*
SBY9650	*H3 P30A*
SBY9651	*H3 S31A*
SBY9652	*H3 T32A*
SBY9653	*H3 G33A*
SBY9654	*H3 G34A*
SBY9655	*H3 V35A*
SBY9656	*H3 K36A*
SBY9657	*H3 K37A*
SBY9658	*H3 P38A*
SBY9659	*H3 H39A*
SBY9660	*H3 R40A*
SBY9662	*H3 K42A*
SBY9663	*H3 P43A*
SBY9664	*H3 G44A*
SBY9665	*H3 T45A*

SBY9666	*H3 V46A*
SBY9667	*H3 A47S*
SBY9668	*H3 L48A*
SBY9669	*H3 R49A*
SBY9670	*H3 E50A*
SBY9671	*H3 I51A*
SBY9672	*H3 R52A*
SBY9673	*H3 R53A*
SBY9674	*H3 F54A*
SBY9675	*H3 Q55A*
SBY9676	*H3 K56A*
SBY9677	*H3 S57A*
SBY9678	*H3 T58A*
SBY9679	*H3 E59A*
SBY9680	*H3 L60A*
SBY9681	*H3 L61A*
SBY9683	*H3 R63A*
SBY9684	*H3 K64A*
SBY9685	*H3 L65A*
SBY9686	*H3 P66A*
SBY9687	*H3 F67A*
SBY9689	*H3 R69A*
SBY9690	*H3 L70A*
SBY9691	*H3 V71A*
SBY9692	*H3 R72A*
SBY9693	*H3 E73A*
SBY9694	*H3 I74A*
SBY9695	*H3 A75S*
SBY9696	*H3 Q76A*
SBY9697	*H3 D77A*
SBY9699	*H3 K79A*
SBY9700	*H3 T80A*
SBY9701	*H3 D81A*
SBY9702	*H3 L82A*
SBY9703	*H3 R83A*
SBY9704	*H3 F84A*
SBY9705	*H3 Q85A*
SBY9706	*H3 S86A*
SBY9707	*H3 S87A*
SBY9708	*H3 A88S*
SBY9709	*H3 G90A*
SBY9710	*H3 A91S*
SBY9711	*H3 L92A*
SBY9712	*H3 Q93A*
SBY9713	*H3 S95A*
SBY9714	*H3 V96A*
SBY9715	*H3 A98S*
SBY9716	*H3 Y99A*
SBY9717	*H3 L100A*
SBY9718	*H3 V101A*
SBY9719	*H3 S102A*
SBY9720	*H3 F104A*
SBY9721	*H3 E105A*
SBY9722	*H3 D106A*
SBY9723	*H3 T107A*
SBY9724	*H3 N108A*
SBY9725	*H3 L109A*
SBY9726	*H3 A110S*
SBY9727	*H3 A111S*
SBY9728	*H3 A114S*
SBY9729	*H3 K115A*
SBY9730	*H3 V117A*

SBY9731 *H3 Q120A*
SBY9732 *H3 K121A*
SBY9733 *H3 K122A*
SBY9734 *H3 I124A*
SBY9735 *H3 K125A*
SBY9736 *H3 L126A*
SBY9737 *H3 A127S*
SBY9738 *H3 R128A*
SBY9739 *H3 R129A*
SBY9740 *H3 L130A*
SBY9741 *H3 R131A*
SBY9742 *H3 G132A*
SBY9743 *H3 E133A*
SBY9744 *H3 R134A*
SBY9745 *H3 S135A*
SBY9746 *H4 S1A*
SBY9747 *H4 G2A*
SBY9748 *H4 R3A*
SBY9749 *H4 G4A*
SBY9750 *H4 K5A*
SBY9751 *H4 G6A*
SBY9752 *H4 G7A*
SBY9753 *H4 K8A*
SBY9754 *H4 L10A*
SBY9755 *H4 G11A*
SBY9756 *H4 K12A*
SBY9757 *H4 G13A*
SBY9758 *H4 G14A*
SBY9759 *H4 A15S*
SBY9760 *H4 K16A*
SBY9761 *H4 R17A*
SBY9762 *H4 H18A*
SBY9763 *H4 R19A*
SBY9764 *H4 K20A*
SBY9765 *H4 I21A*
SBY9766 *H4 L22A*
SBY9767 *H4 R23A*
SBY9768 *H4 D24A*
SBY9769 *H4 N25A*
SBY9770 *H4 I26A*
SBY9771 *H4 Q27A*
SBY9772 *H4 G28A*
SBY9773 *H4 I29A*
SBY9774 *H4 T30A*
SBY9775 *H4 K31A*
SBY9776 *H4 P32A*
SBY9777 *H4 A33S*
SBY9778 *H4 I34A*
SBY9779 *H4 R35A*
SBY9780 *H4 R36A*
SBY9781 *H4 L37A*
SBY9782 *H4 A38S*
SBY9783 *H4 G41A*
SBY9784 *H4 G42A*
SBY9785 *H4 V43A*
SBY9786 *H4 K44A*
SBY9787 *H4 I46A*
SBY9788 *H4 S47A*
SBY9789 *H4 G48A*
SBY9790 *H4 L49A*
SBY9791 *H4 I50A*
SBY9792 *H4 Y51A*

SBY9793	*H4 E52A*
SBY9919	*H4 E53A*
SBY9794	*H4 V54A*
SBY9795	*H4 R55A*
SBY9796	*H4 A56S*
SBY9797	*H4 V57A*
SBY9798	*H4 L58A*
SBY9799	*H4 K59A*
SBY9800	*H4 S60A*
SBY9801	*H4 F61A*
SBY9802	*H4 E63A*
SBY9803	*H4 S64A*
SBY9804	*H4 V65A*
SBY9805	*H4 I66A*
SBY9806	*H4 R67A*
SBY9807	*H4 D68A*
SBY9808	*H4 S69A*
SBY9809	*H4 V70A*
SBY9810	*H4 T71A*
SBY9811	*H4 Y72A*
SBY9812	*H4 T73A*
SBY9813	*H4 E74A*
SBY9814	*H4 H75A*
SBY9815	*H4 K77A*
SBY9816	*H4 K79A*
SBY9817	*H4 T80A*
SBY9818	*H4 V81A*
SBY9819	*H4 T82A*
SBY9820	*H4 S83A*
SBY9821	*H4 D85A*
SBY9822	*H4 V86A*
SBY9823	*H4 V87A*
SBY9824	*H4 Y88A*
SBY9825	*H4 A89S*
SBY9826	*H4 L90A*
SBY9827	*H4 R92A*
SBY9828	*H4 Q93A*
SBY9829	*H4 G94A*
SBY9830	*H4 R95A*
SBY9831	*H4 T96A*
SBY9832	*H4 Y98A*
SBY9833	*H4 G99A*
SBY9834	*H4 F100A*
SBY9835	*H4 G101A*
SBY9836	*H4 G102A*

Strain	Genotype
SBY4	*MATα ura3-1 leu2-3,112 his3-11 trp1-1 can1-100 ade2-1 bar1-1*
SBY719	*MATa ura3-1 leu2-3,112 his3-11:pCUP1GFP12-LacI12:HIS chr8:CEN-lacO:TRP1 can1-100 ade2-1 bar1-1*
SBY9837	*MATa ura3-1 leu2-3,112 his3-11:pCUP1GFP12-LacI12:HIS chr8:CEN-lacO:TRP1 can1-100 ade2-1:7-tetOp-Ub-R-IPL1:ADE2 bar1-1 lys2Δ ipl1ΔKAN hht1-hhf1ΔHYG HHT2-HHF2 synthetic:URA3*
SBY9838	*MATa ura3-1 leu2-3,112 his3-11:pCUP1GFP12-LacI12:HIS chr8:CEN-lacO:TRP1 can1-100 ade2-1:7-tetOp-Ub-R-IPL1:ADE2 bar1-1 lys2Δ ipl1ΔKAN hht1-hhf1ΔHYG hht2-Q5A-HHF2 synthetic:URA3 PDS1-myc18:LEU2*
SBY9839	*MATa ura3-1 leu2-3,112 his3-11:pCUP1GFP12-LacI12:HIS chr8:CEN-lacO:TRP1 can1-100 ade2-1:7-tetOp-Ub-R-IPL1:ADE2 BAR ipl1ΔKAN hht1-hhf1ΔHYG hht2-R40A-HHF2 synthetic:URA3*
SBY9840	*MATa ura3-1 leu2-3,112 his3-11:pCUP1GFP12-LacI12:HIS chr8:CEN-lacO:TRP1 can1-100*

	ade2-1:7-tetOp-Ub-R-IPL1:ADE2 BAR lys2Δ ipl1ΔKAN hht1-hhf1ΔHYG hht2-G44A-HHF2 synthetic:URA3
SBY9841	*MATa ura3-1 leu2-3,112 his3-11:pCUP1GFP12-LacI12:HIS chr8:CEN-lacO:TRP1 can1-100 ade2-1:7-tetOp-Ub-R-IPL1:ADE2 bar1-1 lys2 ipl1ΔKAN hht1-hhf1ΔHYG hht2-R53A-HHF2 synthetic:URA3*
SBY9842	*MATa ura3-1 leu2-3,112 his3-11:pCUP1GFP12-LacI12:HIS chr8:CEN-lacO:TRP1 can1-100 ade2-1:7-tetOp-Ub-R-IPL1:ADE2 bar1-1 lys2Δ ipl1ΔKAN hht1-hhf1ΔHYG hht2-N108A-HHF2 synthetic:URA3*
SBY9843	*MATa ura3-1 leu2-3,112 his3-11:pCUP1GFP12-LacI12:HIS chr8:CEN-lacO:TRP1 can1-100 ade2-1:7-tetOp-Ub-R-IPL1:ADE2 BAR lys2Δ ipl1ΔKAN hht1-hhf1ΔHYG hht2-L109A-HHF2 synthetic:URA3 PDS1-myc18:LEU2*
SBY9844	*MATa ura3-1 leu2-3,112 his3-11:pCUP1GFP12-LacI12:HIS chr8:CEN-lacO:TRP1 can1-100 ade2-1:7-tetOp-Ub-R-IPL1:ADE2 bar1-1 lys2Δ ipl1ΔKAN hht1-hhf1ΔHYG HHT2-HHF2 synthetic:URA3*
SBY9845	*MATa ura3-1 leu2-3,112 his3-11:pCUP1GFP12-LacI12:HIS chr8:CEN-lacO:TRP1 can1-100 ade2-1:7-tetOp-Ub-R-IPL1:ADE2 bar1-1 lys2Δ ipl1ΔKAN hht1-hhf1ΔHYG HHT2-hhf2-K44A synthetic:URA3*
SBY9846	*MATa ura3-1 leu2-3,112 his3-11:pCUP1GFP12-LacI12:HIS chr8:CEN-lacO:TRP1 can1-100 ade2-1:7-tetOp-Ub-R-IPL1:ADE2 bar1-1 ipl1ΔKAN hht1-hhf1ΔHYG HHT2-hhf2-V81A synthetic:URA3*
SBY9847	*MATa ura3-1 leu2-3,112 his3-11:pCUP1GFP12-LacI12:HIS chr8:CEN-lacO:TRP1 can1-100 ade2-1:7-tetOp-Ub-R-IPL1:ADE2 bar1-1 lys2Δ ipl1ΔKAN hht1-hhf1ΔHYG HHT2-hhf2-Y98A synthetic:URA3*
SBY9848	*MATa ura3-1 leu2-3,112 his3-11:pCUP1GFP12-LacI12:HIS chr8:CEN-lacO:TRP1 can1-100 ade2-1:7-tetOp-Ub-R-IPL1:ADE2 bar1-1 lys2Δ ipl1ΔKAN hht1-hhf1ΔHYG HHT2-HHF2 synthetic:URA3 mad3ΔHIS*
SBY9849	*MATa ura3-1 leu2-3,112 his3-11:pCUP1GFP12-LacI12:HIS chr8:CEN-lacO:TRP1 can1-100 ade2-1:7-tetOp-Ub-R-IPL1:ADE2 bar1-1 lys2Δ ipl1ΔKAN hht1-hhf1ΔHYG hht2-Q5A-HHF2 synthetic:URA3 mad3ΔHIS*
SBY9850	*MATa ura3-1 leu2-3,112 his3-11:pCUP1GFP12-LacI12:HIS chr8:CEN-lacO:TRP1 can1-100 ade2-1:7-tetOp-Ub-R-IPL1:ADE2 BAR ipl1ΔKAN hht1-hhf1ΔHYG hht2-R40A-HHF2 synthetic:URA3 mad3ΔHIS*
SBY9851	*MATa ura3-1 leu2-3,112 his3-11:pCUP1GFP12-LacI12:HIS chr8:CEN-lacO:TRP1 can1-100 ade2-1:7-tetOp-Ub-R-IPL1:ADE2 BAR lys2Δ ipl1ΔKAN hht1-hhf1ΔHYG hht2-G44A-HHF2 synthetic:URA3 mad3ΔHIS*
SBY9852	*MATa ura3-1 leu2-3,112 his3-11:pCUP1GFP12-LacI12:HIS chr8:CEN-lacO:TRP1 can1-100 ade2-1:7-tetOp-Ub-R-IPL1:ADE2 bar1-1 ipl1ΔKAN hht1-hhf1ΔHYG hht2-R53A-HHF2 synthetic:URA3 mad3ΔHIS*
SBY9853	*MATa ura3-1 leu2-3,112 his3-11:pCUP1GFP12-LacI12:HIS chr8:CEN-lacO:TRP1 can1-100 ade2-1:7-tetOp-Ub-R-IPL1:ADE2 bar1-1 ipl1ΔKAN hht1-hhf1ΔHYG hht2-N108A-HHF2 synthetic:URA3 mad3ΔHIS*
SBY9854	*MATa ura3-1 leu2-3,112 his3-11:pCUP1GFP12-LacI12:HIS chr8:CEN-lacO:TRP1 can1-100 ade2-1:7-tetOp-Ub-R-IPL1:ADE2 BAR ipl1ΔKAN hht1-hhf1ΔHYG hht2-L109A-HHF2 synthetic:URA3 mad3ΔHIS*
SBY9855	*MATa ura3-1 leu2-3,112 his3-11:pCUP1GFP12-LacI12:HIS chr8:CEN-lacO:TRP1 can1-100 ade2-1:7-tetOp-Ub-R-IPL1:ADE2 bar1-1 ipl1ΔKAN hht1-hhf1ΔHYG HHT2-HHF2 synthetic:URA3 mad3ΔHIS*
SBY9856	*MATa ura3-1 leu2-3,112 his3-11:pCUP1GFP12-LacI12:HIS chr8:CEN-lacO:TRP1 can1-100 ade2-1:7-tetOp-Ub-R-IPL1:ADE2 bar1-1 lys2Δ ipl1ΔKAN hht1-hhf1ΔHYG HHT2-hhf2-K44A synthetic:URA3 mad3ΔHIS*
SBY9857	*MATa ura3-1 leu2-3,112 his3-11:pCUP1GFP12-LacI12:HIS chr8:CEN-lacO:TRP1 can1-100 ade2-1:7-tetOp-Ub-R-IPL1:ADE2 bar1-1 ipl1ΔKAN hht1-hhf1ΔHYG HHT2-hhf2-V81A synthetic:URA3 mad3ΔHIS*
SBY9858	*MATa ura3-1 leu2-3,112 his3-11:pCUP1GFP12-LacI12:HIS chr8:CEN-lacO:TRP1 can1-100 ade2-1:7-tetOp-Ub-R-IPL1:ADE2 bar1-1 ipl1ΔKAN hht1-hhf1ΔHYG HHT2-hhf2-Y98A synthetic:URA3 mad3ΔHIS*
SBY9870	*MATa ura3-1 leu2-3,112 his3-11:pCUP1GFP12-LacI12:HIS trp1-1:lacO:TRP1 can1-100 ade2-1:7-tetOp-Ub-R-IPL1:ADE2 hht1-hhf1ΔHYG HHT2-HHF2 synthetic:URA3 [pRS425, LEU2, 2 μ]*
SBY9871	*MATa ura3-1 leu2-3,112 his3-11:pCUP1GFP12-LacI12:HIS trp1-1:lacO:TRP1 can1-100 ade2-1:7-tetOp-Ub-R-IPL1:ADE2 hht1-hhf1ΔHYG HHT2-HHF2 synthetic:URA3 [pSB1780; SGO1,LEU2, 2 μ]*

SBY9874	*MATa ura3-1::NAT leu2-3,112 his3-11:pCUP1-GFP12-LacI12:HIS3 trp1-1:lacO:TRP1 ipl1ΔKAN can1-100 ade2-1:7-tetOp-Ub-R-IPL1:ADE2 hht1-hhf1ΔHYG hht2-R40A-HHF2 synthetic:URA3 [pRS425, LEU2, 2 μ]*
SBY9875	*MATa ura3-1::NAT leu2-3,112 his3-11:pCUP1GFP12-LacI12:HIS trp1-1:lacO:TRP1 ipl1ΔKAN can1-100 ade2-1:7-tetOp-Ub-R-IPL1:ADE2 hht1-hhf1ΔHYG hht2-R40A-HHF2 synthetic:URA3 [pSB1780; SGO1,LEU2, 2 μ]*
SBY9876	*MATa ura3-1::NAT leu2-3,112 his3-11:pCUP1GFP12-LacI12:HIS trp1-1:lacO:TRP1 ipl1ΔKAN can1-100 ade2-1:7-tetOp-Ub-R-IPL1:ADE2 hht1-hhf1ΔHYG hht2-G44A-HHF2 synthetic:URA3 [pRS425, LEU2, 2 μ]*
SBY9877	*MATa ura3-1::NAT leu2-3,112 his3-11:pCUP1GFP12-LacI12:HIS trp1-1:lacO:TRP1 ipl1ΔKAN can1-100 ade2-1:7-tetOp-Ub-R-IPL1:ADE2 hht1-hhf1ΔHYG hht2-G44A-HHF2 synthetic:URA3 [pSB1780; SGO1,LEU2, 2 μ]*
SBY9880	*MATa ura3-1 leu2-3,112 his3-11:pCUP1GFP12-LacI12:HIS chr8:CEN-lacO:TRP1 can1-100 ade2-1 hht1-hhf1ΔHYG hht2-Q5A-HHF2 synthetic:URA3*
SBY9881	*MATa ura3-1 leu2-3,112 his3-11:pCUP1GFP12-LacI12:HIS chr8:CEN-lacO:TRP1 can1-100 ade2-1 lys2Δ hht1-hhf1ΔHYG hht2-R40A-HHF2 synthetic:URA3*
SBY9882	*MATa ura3-1 leu2-3,112 his3-11:pCUP1GFP12-LacI12:HIS chr8:CEN-lacO:TRP1 can1-100 ade2-1 lys2Δ hht1-hhf1ΔHYG hht2-G44A-HHF2 synthetic:URA3*
SBY9883	*MATa ura3-1 leu2-3,112 his3-11:pCUP1GFP12-LacI12:HIS chr8:CEN-lacO:TRP1 can1-100 ade2-1 lys2Δ hht1-hhf1ΔHYG hht2-R53A-HHF2 synthetic:URA3*
SBY9884	*MATa ura3-1 leu2-3,112 his3-11:pCUP1GFP12-LacI12:HIS chr8:CEN-lacO:TRP1 can1-100 ade2-1 lys2Δ hht1-hhf1ΔHYG hht2-N108A-HHF2 synthetic:URA3*
SBY9885	*MATa ura3-1 leu2-3,112 his3-11:pCUP1GFP12-LacI12:HIS chr8:CEN-lacO:TRP1 can1-100 ade2-1 lys2Δ hht1-hhf1ΔHYG hht2-L109A-HHF2 synthetic:URA3*
SBY9886	*MATa ura3-1 leu2-3,112 his3-11:pCUP1GFP12-LacI12:HIS chr8:CEN-lacO:TRP1 can1-100 ade2-1 hht1-hhf1ΔHYG HHT2-hhf2-K44A synthetic:URA3 PDS1-myc18:LEU2*
SBY9887	*MATa ura3-1 leu2-3,112 his3-11:pCUP1GFP12-LacI12:HIS chr8:CEN-lacO:TRP1 can1-100 ade2-1 hht1-hhf1ΔHYG HHT2-hhf2-V81A synthetic:URA3*
SBY9888	*MATa ura3-1 leu2-3,112 his3-11:pCUP1GFP12-LacI12:HIS chr8:CEN-lacO:TRP1 can1-100 ade2-1 hht1-hhf1ΔHYG HHT2-hhf2-Y98A synthetic:URA3*
SBY10182	*MATa ura3-1 leu2,3-112:: pCMV-LacI-3FLAG::LEU2 his3-11 trp1-1 ade2-1:7-tetOp-Ub-R-IPL1:ADE2 bar1-1 ipl1ΔKAN can1-100 LYS2 hht1-hhf1ΔHYG hht2-R40A-HHF2 synthetic:URA3 [pSB963, WT Minichromosome ,CEN3, LacO, TRP1]*
SBY10183	*MATa ura3-1 leu2,3-112:: pCMV-LacI-3FLAG::LEU2 his3-11 trp1-1 ade2-1:7-tetOp-Ub-R-IPL1:ADE2 bar1-1 ipl1ΔKAN can1-100 LYS2 hht1-hhf1ΔHYG hht2-L109A-HHF2 synthetic:URA3 [pSB963, WT Minichromosome ,CEN3, LacO, TRP1]*
SBY10184	*MATa ura3-1 leu2,3-112:: pCMV-LacI-3FLAG::LEU2 his3-11 trp1-1 ade2-1:7-tetOp-Ub-R-IPL1:ADE2 bar1-1 ipl1ΔKAN can1-100 LYS2 hht1-hhf1ΔHYG HHT2-HHF2 synthetic:URA3 [pSB963, WT Minichromosome ,CEN3, LacO, TRP1]*
SBY10185	*MATa ura3-1 leu2,3-112:: pCMV-LacI-3FLAG::LEU2 his3-11 trp1-1 ade2-1:7-tetOp-Ub-R-IPL1:ADE2 bar1-1 ipl1ΔKAN can1-100 LYS2 hht1-hhf1ΔHYG HHT2-HHF2 synthetic:URA3 [pSB963, WT Minichromosome ,CEN3, LacO, TRP1]*
SBY10186	*MATa ura3-1 leu2,3-112:: pCMV-LacI-3FLAG::LEU2 his3-11 trp1-1 ade2-1:7-tetOp-Ub-R-IPL1:ADE2 bar1-1 ipl1ΔKAN can1-100 LYS2 hht1-hhf1ΔHYG hht2-N108A-HHF2 synthetic:URA3 [pSB963, WT Minichromosome ,CEN3, LacO, TRP1]*
SBY10187	*MATa ura3-1 leu2,3-112:: pCMV-LacI-3FLAG::LEU2 his3-11 trp1-1 ade2-1:7-tetOp-Ub-R-IPL1:ADE2 bar1-1 ipl1ΔKAN can1-100 LYS2 hht1-hhf1ΔHYG hht2-R53A-HHF2 synthetic:URA3 [pSB963, WT Minichromosome ,CEN3, LacO, TRP1]*
SBY10188	*MATa ura3-1 leu2,3-112:: pCMV-LacI-3FLAG::LEU2 his3-11 trp1-1 ade2-1:7-tetOp-Ub-R-IPL1:ADE2 bar1-1 ipl1ΔKAN can1-100 LYS2 hht1-hhf1ΔHYG hht2-G44A-HHF2 synthetic:URA3 [pSB963, WT Minichromosome ,CEN3, LacO, TRP1]*
SBY10189	*MATa ura3-1 leu2,3-112:: pCMV-LacI-3FLAG::LEU2 his3-11 trp1-1 ade2-1:7-tetOp-Ub-R-IPL1:ADE2 bar1-1 ipl1ΔKAN can1-100 LYS2 hht1-hhf1ΔHYG HHT2-hhf2-K44A synthetic:URA3 [pSB963, WT Minichromosome ,CEN3, LacO, TRP1]*
SBY10190	*MATa ura3-1 leu2,3-112:: pCMV-LacI-3FLAG::LEU2 his3-11 trp1-1 ade2-1:7-tetOp-Ub-R-IPL1:ADE2 bar1-1 ipl1ΔKAN can1-100 LYS2 hht1-hhf1ΔHYG HHT2-hhf2-V81A synthetic:URA3 [pSB963, WT Minichromosome ,CEN3, LacO, TRP1]*
SBY10191	*MATa ura3-1 leu2,3-112:: pCMV-LacI-3FLAG::LEU2 his3-11 trp1-1 ade2-1:7-tetOp-Ub-R-IPL1:ADE2 bar1-1 ipl1ΔKAN can1-100 LYS2 hht1-hhf1ΔHYG HHT2-hhf2-Y98A synthetic:URA3 [pSB963, WT Minichromosome ,CEN3, LacO, TRP1]*
SBY10192	*MATa ura3-1 leu2,3-112:: pCMV-LacI-3FLAG::LEU2 his3-11 trp1-1 ade2-1:7-tetOp-Ub-R-IPL1:ADE2 bar1-1 ipl1ΔKAN can1-100 LYS2 hht1-hhf1ΔHYG hht2-Q5A-HHF2 synthetic:URA3*

	[pSB963, WT Minichromosome ,CEN3, LacO, TRP1]
SBY10284	*MATa ura3-1::NAT leu2-3,112 his3-11:pCUP1GFP12-LacI12:HIS trp1-1:lacO:TRP1 ipl1ΔKAN can1-100 ade2-1:7-tetOp-Ub-R-IPL1:ADE2 hht1-hhf1ΔHYG hht2-Q5A-HHF2 synthetic:URA3 [pRS425, LEU2, 2 μ]*
SBY10285	*MATa ura3-1::NAT leu2-3,112 his3-11:pCUP1GFP12-LacI12:HIS trp1-1:lacO:TRP1 ipl1ΔKAN can1-100 ade2-1:7-tetOp-Ub-R-IPL1:ADE2 hht1-hhf1ΔHYG hht2-Q5A-HHF2 synthetic:URA3 [pSB1780; SGO1,LEU2, 2 μ]*
SBY10286	*MATa ura3-1::NAT leu2-3,112 his3-11:pCUP1GFP12-LacI12:HIS trp1-1:lacO:TRP1 ipl1ΔKAN can1-100 ade2-1:7-tetOp-Ub-R-IPL1:ADE2 hht1-hhf1ΔHYG hht2-R53A-HHF2 synthetic:URA3 [pRS425, LEU2, 2 μ]*
SBY10287	*MATa ura3-1::NAT leu2-3,112 his3-11:pCUP1GFP12-LacI12:HIS trp1-1:lacO:TRP1 ipl1ΔKAN can1-100 ade2-1:7-tetOp-Ub-R-IPL1:ADE2 hht1-hhf1ΔHYG hht2-R53A-HHF2 synthetic:URA3 [pSB1780; SGO1,LEU2, 2 μ]*
SBY10288	*MATa ura3-1::NAT leu2-3,112 his3-11:pCUP1GFP12-LacI12:HIS trp1-1:lacO:TRP1 ipl1ΔKAN can1-100 ade2-1:7-tetOp-Ub-R-IPL1:ADE2 hht1-hhf1ΔHYG hht2-N108A-HHF2 synthetic:URA3 [pRS425, LEU2, 2 μ]*
SBY10289	*MATa ura3-1::NAT leu2-3,112 his3-11:pCUP1GFP12-LacI12:HIS trp1-1:lacO:TRP1 ipl1ΔKAN can1-100 ade2-1:7-tetOp-Ub-R-IPL1:ADE2 hht1-hhf1ΔHYG hht2-N108A-HHF2 synthetic:URA3 [pSB1780; SGO1,LEU2, 2 μ]*
SBY10290	*MATa ura3-1::NAT leu2-3,112 his3-11:pCUP1GFP12-LacI12:HIS trp1-1:lacO:TRP1 ipl1ΔKAN can1-100 ade2-1:7-tetOp-Ub-R-IPL1:ADE2 hht1-hhf1ΔHYG hht2-L109A-HHF2 synthetic:URA3 [pRS425, LEU2, 2 μ]*
SBY10291	*MATa ura3-1::NAT leu2-3,112 his3-11:pCUP1GFP12-LacI12:HIS trp1-1:lacO:TRP1 ipl1ΔKAN can1-100 ade2-1:7-tetOp-Ub-R-IPL1:ADE2 hht1-hhf1ΔHYG hht2-L109A-HHF2 synthetic:URA3 [pSB1780; SGO1,LEU2, 2 μ]*
SBY10292	*MATa ura3-1::NAT leu2-3,112 his3-11:pCUP1GFP12-LacI12:HIS trp1-1:lacO:TRP1 ipl1ΔKAN can1-100 ade2-1:7-tetOp-Ub-R-IPL1:ADE2 hht1-hhf1ΔHYG HHT2-hhf2-K44A synthetic:URA3 [pRS425, LEU2, 2 μ]*
SBY10293	*MATa ura3-1::NAT leu2-3,112 his3-11:pCUP1GFP12-LacI12:HIS trp1-1:lacO:TRP1 ipl1ΔKAN can1-100 ade2-1:7-tetOp-Ub-R-IPL1:ADE2 hht1-hhf1ΔHYG HHT2-hhf2-K44A synthetic:URA3 [pSB1780; SGO1,LEU2, 2 μ]*
SBY10294	*MATa ura3-1::NAT leu2-3,112 his3-11:pCUP1GFP12-LacI12:HIS trp1-1:lacO:TRP1 ipl1ΔKAN can1-100 ade2-1:7-tetOp-Ub-R-IPL1:ADE2 hht1-hhf1ΔHYG HHT2-hhf2-V81A synthetic:URA3 [pRS425, LEU2, 2 μ]*
SBY10295	*MATa ura3-1::NAT leu2-3,112 his3-11:pCUP1GFP12-LacI12:HIS trp1-1:lacO:TRP1 ipl1ΔKAN can1-100 ade2-1:7-tetOp-Ub-R-IPL1:ADE2 hht1-hhf1ΔHYG HHT2-hhf2-V81A synthetic:URA3 [pSB1780; SGO1,LEU2, 2 μ]*
SBY10296	*MATa ura3-1::NAT leu2-3,112 his3-11:pCUP1GFP12-LacI12:HIS trp1-1:lacO:TRP1 ipl1ΔKAN can1-100 ade2-1:7-tetOp-Ub-R-IPL1:ADE2 hht1-hhf1ΔHYG HHT2-hhf2-Y98A synthetic:URA3 [pRS425, LEU2, 2 μ]*
SBY10297	*MATa ura3-1::NAT leu2-3,112 his3-11:pCUP1GFP12-LacI12:HIS trp1-1:lacO:TRP1 ipl1ΔKAN can1-100 ade2-1:7-tetOp-Ub-R-IPL1:ADE2 hht1-hhf1ΔHYG HHT2-hhf2-Y98A synthetic:URA3 [pSB1780; SGO1,LEU2, 2 μ]*
SBY11682	*MATα ura3-1 leu2-3,112 his3-11 trp1-1 can1-100 ade2-1 bar1-1 orc2-1*